PERFORMANCE BASED DESIGN OF CIRCULAR SCRAP TYRE PAD ISOLATOR BY MACHINE LEARNING

THESIS REPORT

Submitted by

ANANDHAKRISHNAN M

TKM21CESC02

to

the A P J Abdul Kalam Technological University

in partial fulfilment of the requirements for the award of the Degree

of

Master of Technology

in

Structural Engineering & Construction Management

DEPARTMENT OF CIVIL ENGINEERING

TKM College of Engineering, Kollam

MAY 2023

DECLARATION

I undersigned hereby declare that the project report, "**Performance Based Design of Circular Scrap Tyre Pad Isolator by Machine Learning**", submitted for partial fulfilment of the requirements for the award of the degree of Master of Technology of the APJ Abdul Kalam Technological University, Kerala is a bonafide work done by me under supervision of **Mr Asif Basheer,** Assistant Professor, Department of Civil Engineering. This submission represents my ideas in my own words and where ideas or words of others have been included; I have adequately and accurately cited and referenced the original sources. I also declare that I have adhered to ethics of academic honesty and integrity and have not misrepresented or fabricated any data or idea or fact or source in my submission. I understand that any violation of the above will be a cause for disciplinary action by the institute and/or the University and can also evoke penal action from the sources which have thus not been properly cited or from whom proper permission has not been obtained. This report has not been previously formed the basis for the award of any degree, diploma or similar title of any other University.

Place: Kollam Anandhakrishnan M

Date: 22-04-2023

DEPARTMENT OF CIVIL ENGINEERING

T.K.M. COLLEGE OF ENGINEERING, KOLLAM

CERTIFICATE

Certified that this report entitled **'Performance Based Design of Circular Scrap Tyre Pad Isolator by Machine Learning'** is the report of project presented by **Anandhakrishnan M, TKM21CESC02** during **2021-2023** in partial fulfilment of the requirements for the award of the Degree of Master of Technology in Structural Engineering & Construction Management of the A P J Abdul Kalam Technological University.

Guide	Project coordinator	Head of the Department
Prof. Asif Basheer	**Dr Kavitha Madhu**	**Dr. Sajeeb R**
Assistant Professor	Associate Professor	Professor
Dept. of Civil Engg.	Dept. of Civil Engg.	Dept. of Civil Engg.

ACKNOWLEDGEMENT

I take this opportunity to express my deep sense of gratitude and sincere thanks to all who helped me to complete the project successfully.

I am deeply indebted to my guide, **Mr. Asif Basheer,** Assistant Professor, Department of Civil Engineering for his excellent guidance, positive criticism and valuable comments.

I am thankful to my project coordinator, **Mrs. Kavitha Madhu,** Associate Professor, Department of Civil Engineering for her constant supervision as well as for providing necessary information regarding the project.

I am greatly thankful to **Dr. Sajeeb R**, Professor and Head of the Department of Civil Engineering, for his kind support.

Finally, I thank my parents and friends who directly and indirectly contributed to the successful completion of my project.

Anandhakrishnan M

ABSTRACT

Base isolation systems have conventionally been used to mitigate the major impacts of earthquakes on the structures and attenuate their seismic responses. The scrap tyre pads are proven to be a material that resists vibrations. The optimal design of the base isolator has a vital role in the performance of a structure in response to an earthquake. Machine learning (ML) methods have been widely applied to predict the outputs of various problems in the structural engineering field. This study focuses on the development of a Machine Learning (ML)-based approach to predict the design of a base isolation system. The base isolator used in the present work is the Scrap Tyre Pad (STP) in a circular configuration. Conventionally, alternate layers of rubber bonded with steel reinforcement are used as isolators. As scrap tires consist of steel reinforcement inside the rubber itself, it can be considered as a cost-effective method. The presence of steel provides substantial vertical stiffness and rubber imparts horizontal flexibility. The eco-friendly Scrap Tyre Pads (STPs) provide several advantages such as low cost, ease of handling, and shear stiffness adjustments. In the present study, experimental evaluation of Circular Scrap Tyre Pads (CSTPs) under compression and cyclic loading is done in different configurations to analyse the structural behaviour of CSTPs as a base isolator. The damper properties obtained from the experiment are numerically analysed using non-linear time history analysis in ETABS to assess the isolator's performance subjected to seismic loading on masonry structures. The data from the numerical evaluation is stored in Machine Learning (ML) database and the ML algorithm is trained to predict the design characteristics of the base isolator for a given structure. The performance of ML algorithms is validated using statistical metrics.

Keywords: Base isolator, Scrap tyre pads, Circular scrap tyre pads, ETABS, Machine learning

CONTENTS

LIST OF FIGURES

LIST OF TABLES

LIST OF ABBREVIATIONS

ANN	Artificial Neural Network
CSTP	Circular Scrap Tyre Pads
LVDT	Linear Variable Differential Transformer
MPa	Mega Pascal
ML	Machine Learning
SREI	Steel-Reinforced Elastomeric Isolator
STP	Scrap Tyre Pads
RF	Random Forest
XG Boosting	Extreme Gradient Boosting

Chapter 1

Introduction

1.1. General

Seismic base isolation is the process of creating a laterally flexible system between the ground and the structure in order to increase the natural time period and minimize seismic pressures brought on the structure by earthquakes. Although the steel-reinforced elastomeric isolator (SREI) is the most common, its application is restricted to big, expensive, and sophisticated structures due to the SREI's high production costs caused by labour-intensive manufacturing and vulcanization processes. Recent earthquakes have shown that unreinforced masonry structures are extremely vulnerable. In the event of moderate to strong earthquakes, the lack of ductility and poor out-of-plane behaviour of the load-bearing walls of these types of buildings causes considerable damage or entire collapse, which results in a significant loss of life and properties. However, this class of buildings with thick walls are very common in different parts of the world because of their higher durability and better thermal insulation. The development of novel, affordable, sustainable solutions is thus required to increase earthquake resistance and resilience. In general, base isolation systems extend the isolated systems natural periods and improve their damping to minimise the propagation of ground motion to the superstructure. The scrap tire pad (STP) made by natural or synthetic rubber and high strength reinforcing cords exhibits substantial vertical stiffness and horizontal flexibility, and these properties can be regarded as suitable for seismic isolators for structures.

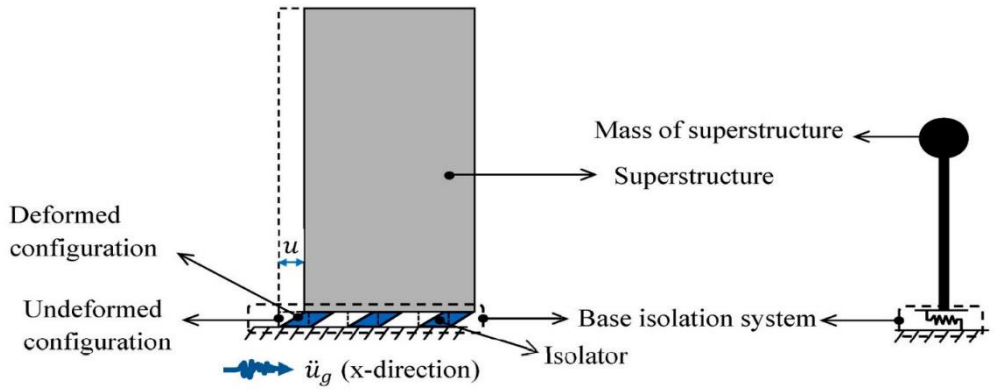

Figure 1.1. Base isolation model (Source: Nguyen et al., 2022)

The optimal design the of base isolator has a vital role in the performance of a structure in response to an earthquake. This study focuses on the development of a Machine Learning (ML) based approach to predict the design of a base isolation system. The base isolator used in the present work is Scrap Tyre Pad (STP) in circular configuration. This study involves the development of a low-cost isolation system for the mitigation of seismic vulnerability of common masonry buildings. For achieving the goal the structural behaviour of the scrap tyre pad isolator has been figured out and the numerical analysis is done on the ETABS software package. Using the results from the numerical analysis a suitable ML model has been generated to predict the design of the system.

1.2. Seismic Isolation

The seismic stresses on structures can be minimized by increasing the fundamental period of the structure or increasing its energy dissipation capabilities. As a result, seismic isolation offers a promising alternative for the design of structures that can withstand earthquakes. Seismic isolation, which has a typically bilinear force-deformation connection, is essentially a means of controlling the seismic response of structures. By placing structural materials with low horizontal stiffness between the structure and the foundation, seismic isolation theoretically decouples the structure from the horizontal components of the ground motion. This results in a fundamental frequency for the structure that is significantly lower than both its fixed-base frequency and the fundamental frequencies of the earthquake ground motion.

1.3. Scrap Tyre Pads

Scrap Tire Pad (STP) is made of natural or synthetic rubber. Steel exhibits substantial vertical stiffness and rubber imparts horizontal flexibility, these properties can be regarded as suitable for seismic isolators for structures. The Eco-friendly Scrap Tyre Pads (STPs) provide several advantages such as low cost, ease of handling and, simple shear stiffness adjustments. Provide environmental benefits, by the reuse of scrap tyres unlike other commercially available base isolators.

Figure 1.2 Scrap tyre (Source: Shirai et al., 2020)

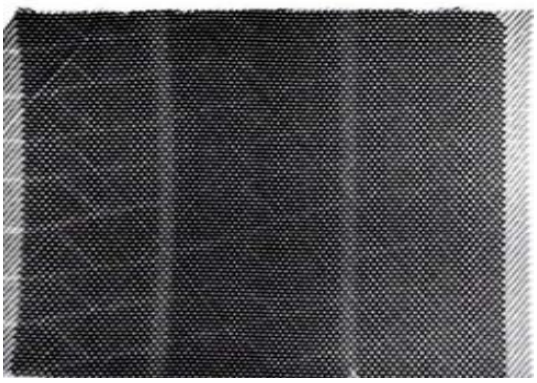

Figure 1.3 X-ray image of Scrap tyre (Source: Shirai et al., 2020)

The concept of using used tyres as elastomeric isolators stem primarily from the fact that automobile tyres are constructed of rubber and feature steel mesh reinforcement in the tread area. In an effort to emulate the behaviour of conventional isolators, Scrap Tire Pad (STP) base isolators are created by stacking layers of scrap tyre thread sections. The rubber-vulcanized wire mesh runs in two nearly orthogonal orientations inside the tyres. Due to the presence of steel mesh inside the tyre layers, the layers that are stacked on top of one another prevent bulging and allow lateral motion, much like standard rubber elastomeric isolators. An STP is obtained by cutting the sidewalls of a used tire to form a tire ring, which is then further divided into equal lengths to obtain tire layers. Each tire layer is then placed on top of each other to form an STP. The horizontal stiffness of an STP can be simply adjusted by changing the number of layers; an increase in the number of layers would make the pad more flexible in the horizontal direction.

1.4. Machine Learning

The fast-growing discipline of data science includes machine learning as a key element. Being a subset of artificial intelligence (AI), machine learning (ML) focuses on using data and algorithms to mimic how people learn while gradually increasing the accuracy of its predictions. Algorithms are trained to make classifications or predictions using statistical techniques, revealing significant insights in data mining projects.

1.4.1. Types of Machine Learning

With respect to the purposes of investigation, ML approaches can broadly be classified into three categories supervised, unsupervised, and reinforcement learning. Using labelled training datasets, supervised learning algorithms analyse relationships between predictor variables and results, applying the learned rule to create a model for categorising fresh data. In supervised learning, there are two main strategies: classification and

regression. Classification models aim to forecast category outcomes, while regression models aim to forecast continuous outcomes. Using labelled training datasets, supervised learning algorithms analyse relationships between predictor variables and results, applying the learned rule to create a model for categorizing fresh data. In supervised learning, there are two main strategies: classification and regression. Classification models aim to forecast category outcomes, while regression models aim to forecast continuous outcomes. On the other hand, unsupervised learning algorithms are used to elucidate concealed patterns in training data that lack labels. The most commonly used methods for inserting data into previously ambiguous bundles within unsupervised learning are clustering approaches, such as hierarchical clustering, K-means clustering, and Gaussian mixture models. Last but not least, reinforcement learning is programmed to sequentially self-correct from environmental feedback and thereby enhance the general model function without labelling the data.

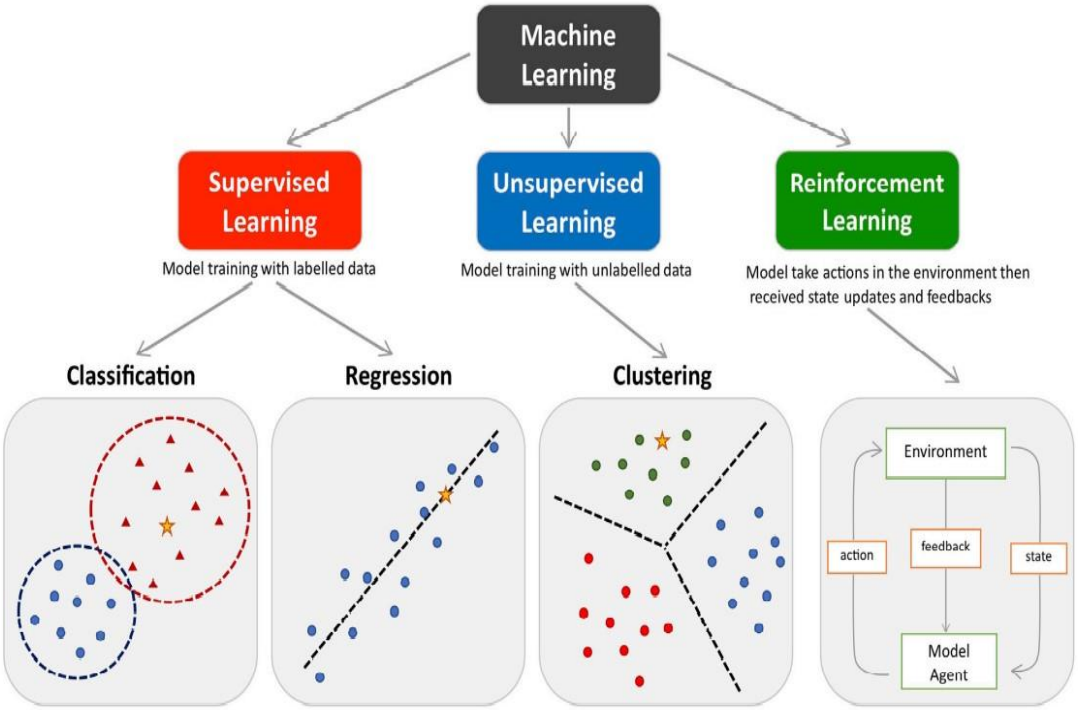

Figure 1.4 Classification of ML techniques (Source: Nguyen et al., 2022)

1.5. Objectives

- To study the load-deformation relation of Circular Scrap Tyre Pads (CSTPs) with different configurations
- To study the variation of stiffness of CSTPs systems with change in shape factor
- To identify changes in the damping factor of CSTPs with different configuration
- To study the effect of vertical pressure of CSTPs systems with change in shape factor
- To predict the required
    - number of dampers,
    - spacing between dampers,
    - time period of the isolated structure,
    - base shear of the isolated structure,
    - best CSTP combination

1.6. Scope

- The study is focusing on experimental analysis of CSTPs with changes in configurations.
- The study is based CSTPs on unbonded conditions.
- Numerical study is conducted on masonry structures.
- Single story, double-story, and triple-story structures are considered.
- Performance analysis of the structure under seismic loading is conducted on the ETABS software package.
- For the prediction of the optimum design of the base isolation system Machine Learning approaches are used.

Chapter:2
Literature Review

2.1. General

An extensive literature study has been conducted for the development of a sustainable base isolation system using STPs. The possibility of the application of machine learning approaches were also investigated. The findings from the literature study is explained in the following sections

2.2. Effectiveness of Base Isolation

Despite being the most widely used, steel-reinforced elastomeric isolators (SREI) have a high production cost due to labor-intensive manufacturing and vulcanization procedures, which limits their use to extremely large, expensive, and complex structures (Kelly et al., 2002, Pan et al., 2005 and May et al., 2002). Matsagar and Jangid, 2008 conducted a study on selected structures using the base isolation technique by use of the layers of isolators at suitable locations. Comparison between different types of isolators, such as elastomeric bearings and sliding systems are evaluated to analyze performance in the retrofitting works done. It is observed that the seismic response of the retrofitted structures reduces significantly in comparison with the conventional structures depicting the effectiveness of the retrofitting done through the base isolation technique. The base isolation system can substantially increase the time period of the structure and can reduce the base shear up to 75% as compared the to fixed one (Tanwer et al.,2019).

2.3. Performance of Steel Rubber Reinforced Base Isolator

Thomas, et al.,2016 studied the analysis of characteristics of steel-rubber base isolators under combined axial tension or compression and base shear by finite element method. The effect of the magnitude and direction of the axial load is investigated for base isolators subject to 375% shear strain. The influence of the number and size of rubber cores in the steel-rubber base isolator is also investigated. From the analysis base isolators with multiple radially-distributed rubber cores were found to be more effective than those with a single central rubber core.

Munoz et al., 2019 conducted a study on rubber tire sheets that are combined with each other by a vulcanization process. Rubber layers with 3mm of layer depth are made of

recycled rubber tire powder in between rubber tire sheets. In between the rubber tire sheet and the steel plate at both ends of the bearing. From the experimental results, a nonlinear hysteretic behavior and energy dissipation were observed, decoupling the lateral movement.

Calabresea et al., 2019, the seismic performance of the Rubber based base-isolated structure is compared to the response of the same building when isolated at the base with conventional devices, namely Laminated Rubber Bearings (LRBs) and Friction Pendulum Systems (FPSs). Studied the high potential of low-cost bearings as base isolation devices for residential buildings.

2.4. Circular Base Isolator

Ohsaki et al.,2015 studied a building frame supported by laminated rubber bearings by finite element analysis and found out that when there is seismic excitation, the vertical pressure changes have a significant impact on the horizontal response force. The circular configuration of the high-damping rubber bearing (HDRB) and lead rubber bearing (LRB) has been modeled and examined in ABAQUS, and the results have been compared with the experimental findings of other researchers.(Saedniya and Talaeitaba, 2019). Rubber Bearings being hyperelastic material have totally reversible force-displacement behavior (Saedniya and Talaeitaba, 2019, Jabbareh et al., 2014). Evaluation of the physical characteristics of sliding-type circular isolators reveals improved performance (Kawamura et al.,2021).

2.5. Mechanical Properties of Scrap Tyre Pads

Mishra et al., 2012, studied the mechanical properties of STP and find out that the vertical stiffness of the STRP isolator is sufficient to withstand the structural weight load of buildings as well as to prevent the lateral forces of the structure. The study suggests the hat ratio between vertical stiffness and horizontal stiffness is above 150 (Eurocode 8 2004). The scrap tire rubber pad (STRP) made by natural or synthetic rubber and high strength reinforcing cords exhibits substantial vertical stiffness and horizontal flexibility (Turer et al., 2008) and these properties can be regarded as suitable for seismic isolators for structures (Zisan and Igarashi, 2021).

2.6. Significance of Unbonded Configuration

From the studies conducted by Topachi et al., 2011 and Sistla and Mohan et al.,2021 on unbonded and bonded configurations found that because of the roll-over deformation

occurring in the unbonded system, a much longer time period can be achieved due to the reduction in the contact area. After the full rollover, there is an abrupt increase in stiffness that serves as a safety mechanism against large displacements during earthquakes. The rollover deformation also offers less stress demand on rubber material. Hence, the peeling stress on the interface between rubber and fibre will be considerably reduce (Pauletta et al ., 2015).

2.7. Analytical Evaluation of Scrap Tyre Pads

Jennifer and Suppiah, 2021 studied the performance of three-story shear frame which is isolated at the base with Scrap Tire Pad (STP) bearings has been analyzed. The response of this structure has been compared with that of an identical structure having a fixed base (ie, without isolation). The natural frequencies and mode shapes have been computed through MATLAB and are compared. The response of the two cases showed that the base isolation by means of STPs is very effective in the fundamental mode of vibration. Zisan, et al., 2021 conducted Finite element analyses of unbonded square and strip-shaped STP isolators which are subjected to the combined effect of axial and lateral loads to investigate their lateral deformation performance under earthquake. They studied the effect of the length-to-width ratio and bearing height on the isolator performance in terms of the force-displacement relationship, horizontal stiffness, damping, and isolation periods.

2.8. Numerical Analysis on Masonry Buildings

The introduction of unbounded fibre-reinforced elastomeric isolators (U-FREIs) found to be very effective in reduction of the seismic vulnerability of low-rise masonry buildings (Deb et al.,2018, Dao et al.,

2020). Deb et al.,2021 from the studies found out considerable reduction in the seismic vulnerability of the base isolated building as compared to that of the fixed base building is observed from the comparison of the analytical fragility curves. Transmissibility of peak ground acceleration to the test model is reduced to a large extent and therefore, peak floor accelerations are of the order of 12%–15% of the peak Table accelerations (Deb et al.,2021).

2.9. Machine Learning

A computationally efficient procedure for developing fragility curves associated with different limit-states of 3D reinforced concrete buildings is proposed (Mitroppoulu and

Papadrakakis,2011). Kiani et al.,2019 from the study figures out that Machine learning can be used as a effective method in deriving the curves is a key step in seismic risk assessment within the performance-based earthquake engineering framework. Neural networks can learn general relations (attenuation and site effects) for estimating earthquake magnitudes directly from raw single-station waveforms (Mousavi and Beroza et al.,2019). Nguyen et al.,2022 studied application of ML to the estimation of the responses of seismic isolation systems in practical design found out that ML methods like Artificial Neural Network and Random forest can effectively predict the response.

2.10. Literature Summary

- Need of base isolation has been studied
- The properties of conventional steel rubber bearings has been studied
- Effect of steel and rubber in conventional base isolator
- Observation on finite element analysis of buildings with base isolator
- Mechanical properties of scrap tyre pads
- Numerical analysis of base isolators in response to earthquake
- Design of base isolation system
- Optimization techniques for base isolators
- Machine Learning approaches

2.11. Gaps Identified

- Machine learning approaches are not implemented in design of base isolation system
- Studies had been conducted on the variation of stiffness with vertical load on conventional steel rubber bearings but have not in case of Scrap Tire Pad (STPs)
- Currently no studies have been conducted on Circular Scrap Tire Pad (CSTP)
- Numerical analysis of buildings isolated with CSTPs are not yet conducted

Chapter 3
Methodology

3.1. General

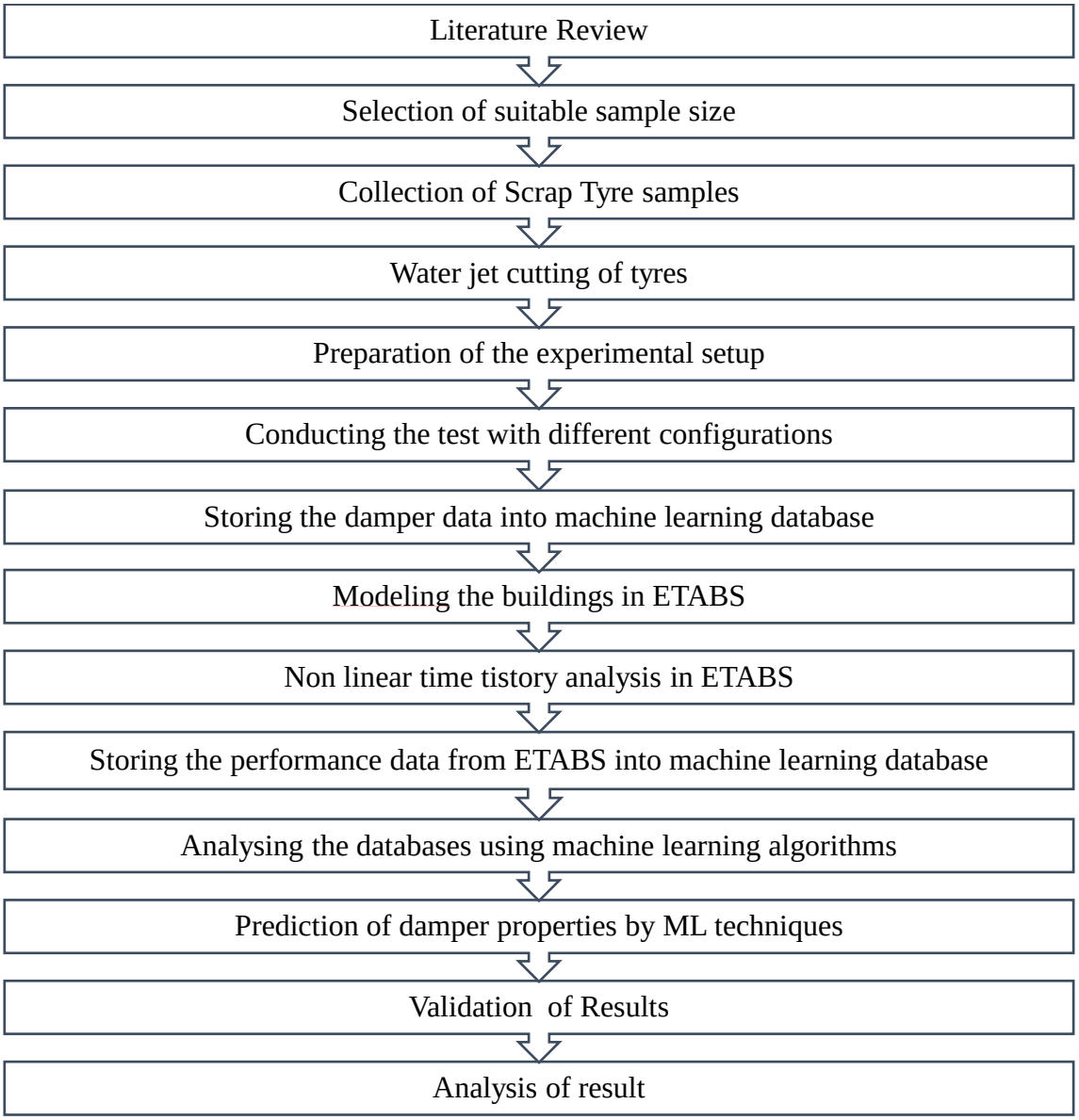

Figure 3.1. Methodology of the study

The methodology followed in the project is illustrated in Figure 3.1. An extensive literature review is done based on the need and application of various base isolator systems. From the literature study, it is understood that low-cost base isolation by STPs can be employed as an effective method in controlling the effect of earthquakes in

superstructures. But to design an isolator it is important to figure out the parameters like damping ratio, horizontal and vertical stiffness of the isolator. Thus, to analyse the parameters experimental study on the STPs under compression and cyclic loading has to be done. Suitable sample size is selected based on the availability of tyre. After fixing the size, the tire sample has been collected. The samples are made into the required dimensions by means of water jet cutting. An experimental set up as discussed in section 4 is prepared and the testing is done with the samples. The damper properties has to be used for the numerical analysis on ETABS. By observing the performance, the damper properties, building properties and corresponding output results, a dataset has to be prepared for Machine Learning modelling. Using this dataset, training and testing of the machine learning algorithm can be done and it is used to predict the damper properties for a proposed design of building.

3.2. Specimen Details

Figure 3.2 Circular scrap tyre specimen

The standard sized tyres of 185/65/R15 is used for the experiment. The width is 185 millimetres and the aspect ratio of tyre is 65, it is the ratio in the percentage of side height to its width and 15 represents the inner circle diameter of the tyre in inches. The sample is made to circles of diameter 145cm by using water jet cutting. The average thickness of the selected sample is measured by using vernier calliper and is known to be 9.6mm. Figure 3.2 represents CSTP the specimen used in the study.

Chapter:4
Experimental Setup

4.1 General

The scrap tyre samples are made into circular shape and are packed one over the other without any bonding agents. For compression testing, the number of layers is increased to study the compression characteristics with a change in shape factor. In the case of cyclic load testing, the shape factor is varied in the same manner as explained and its behaviour is analysed for 1 MPa, 2 MPa and 3 MPa pressure cases.

4.2 Compression Testing

In a computer-controlled universal testing apparatus, isolator specimens were subjected to compression tests (Figure 4.1 and 4.2). STPs are equipped with two steel plates at the top and bottom to evenly distribute the applied load. The specimen was loaded to approximately 300 kN of force. The load at which the breaking sound of the steel strand observed is taken as the breaking load of the sample. After each trial, specimens were replaced with a fresh batch. Using software created by Fuel Instruments and Engineers Pvt. Ltd., the corresponding load and deformation were recorded digitally on a computer.

Figure 4.1 Experimental Setup for compression testing

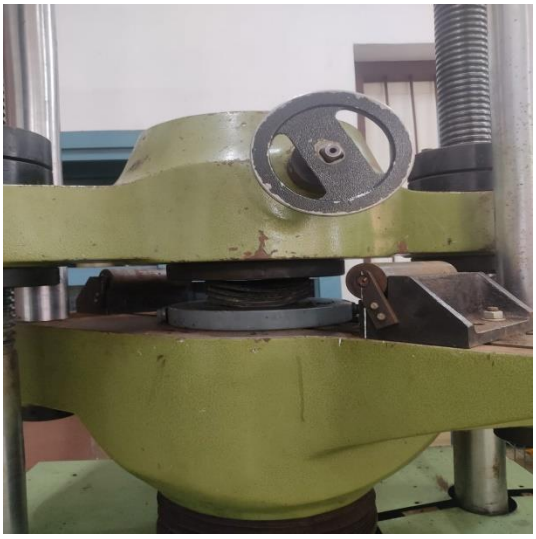

Figure 4.1. STP specimen loaded in the compression machine

The shape factor is an important parameter of the isolator that depends on the height of the isolator specimen, hence the plan area of the considered specimen is kept constant. The height of the specimen can be increased by increasing the no of layers. The number of layers of the considered samples and the corresponding shape factor is shown in Table 4 -1.

Table 4.1. Number of layers vs shape factor

Number of Layers	Shape Factor
4	0.944
6	0.6293
8	0.472
10	0.3776

4.2.1 Procedure

1. Place the specimen with a specified number of layers in between two steel plates
2. The specimen is kept on the compression testing machine between two plates
3. Load is applied till 300kN
4. Corresponding load deformation is digitally recorded.
5. The specimen is then replaced by another set of specimens.

4.3 Cyclic Load Test

The shear performance of the CSTP specimen is found by applying constant vertical pressure and noting the lateral load required for corresponding displacements. The study is conducted to analyze the performance under 1 MPa, 2 Mpa and 3 MPa vertical pressures. Keeping the vertical pressure constant, with the use of a push-pull jack horizontal load is applied. Linear Variable Differential Transformer (LVDT) is used for measuring the horizontal displacement corresponding to the load applied and the value of the displacement is obtained by means of a digital displacement indicator. The applied load by the push pull jack can be figured out by the means of load indicator. The experimental setup for cyclic loading is as shown in Figure 4.3 and Figure 4.4.

Figure 4.3. Experimental setup for cyclic loading

Figure 4.4. Indicators to measure the load and deformations

The Figure 4.5 represents the schematic representation of the the cyclic load application where P represents the vertical load and the F represents the horizontal load acting on the specimen. The cyclic loading is applied such that the rate of loading per sec is kept at a uniform rate as shown in Figure 4.6.

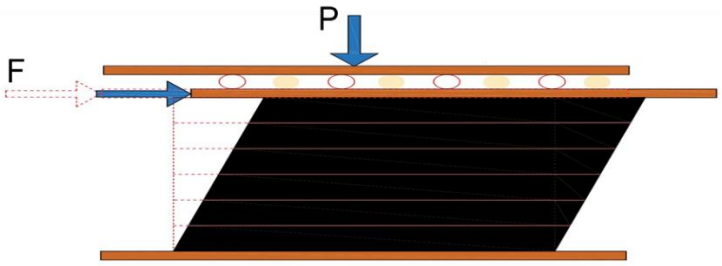

Figure 4.5 Schematic representation of horizontal loading

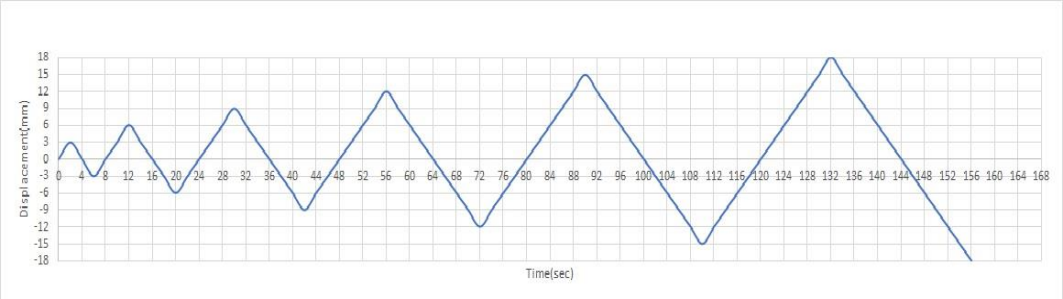

Figure 4.6 Applied horizontal displacement

Figure 4.8 8 layer 2 MPa specimen (+18mm displacement)

Figure 4.9 8 layer 2 MPa specimen

Figure 4.10 8 layer 2 MPa specimen (-18mm displacement)

Figure 4.8, 4.9 and 4.10 represents the behaviour of 8 layer specimen under 2 MPa pressure on cyclic loading action. From the experiment, it is observed that during the horizontal displacement, the specimen is acting as a single unit without any layer separation. Figure 4.8 and 4.10 shows the rollover behaviour of the sample.

4.3.1 Procedure

1. Place the specimen with specified number of layers in between two steel plates

2. The specimen is kept on the loading frame.

3. Above the top plate place rollers of uniform diameter.

4. Place a steel plate above the rollers, one end of the roller is connected to the push-pull jack.

5. Ensure that the rollers are placed correctly so that the vertical load transfer will be uniform.

6. Place the load cell centrally over the assembly to ensure symmetric loading.

7. Connect the load cell to the load indicator.

8. Apply the required vertical load by means of a hydraulic Jack.

9. Set the LVDT to measure the horizontal displacement which is connected to the displacement indicator.

10. Apply cyclic loading by push-pull jack and note down the corresponding load-deformation data.

Chapter:5
Results and Discussion on Experimental Analysis

5.1 General

The shape factor is an important parameter for accessing the properties of the CSTP isolator that depends on the height of the isolator specimen. Hence the study is conducted by keeping the plan area of the considered specimen constant and the height of the specimen is increased by increasing the no of layers. The compression test and cyclic loading test are performed by varying the shape factor.

5.2 Compression Testing

The isolator should be able to withstand and transfer the vertical load of the superstructure above it. Hence it is important to study the compression characteristics of the specimen.

5.2.1 Load Displacement Behavior in Response to Change in Number of Layers

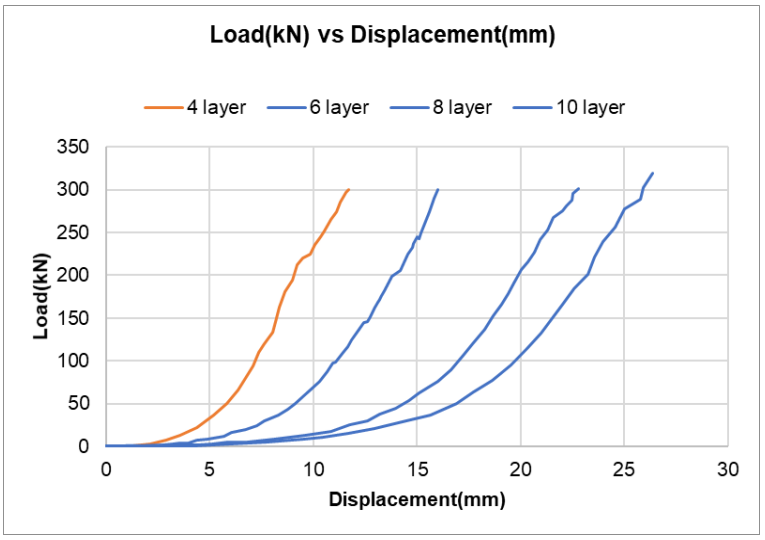

Figure 5.1 Load (kN) vs Displacement (mm) plot

The scrap tyre pads, which were initially somewhat convex in shape, were flattened during the post-loading phase. The stiffness value is low in the initial stage before the application of load which is due to the initial curved shape of the tyre pads. After a certain loading the stiffness of the isolator is improved considerably in all cases under consideration. The slope of the curves seen decreasing with increase in number of layers. The 4 Layer sample had the highest slope which shows that the isolator had behaved more

rigidly. It is observed that even after the sound of breakage is noted from the sample, the specimens were performing well under the action of loading.

5.2.2 Effect of Shape Factor on Vertical Stiffness

The slope of the linear portion in the plot provides the vertical stiffness of CSTP specimen as shown in Figure 5.3. The slope of the specimen with change in shape factor is found to understand the effect of shape factor in vertical stiffness. The 10-layer sample with a shape factor of 0.377 found to have the least stiffness among the all cases under consideration. A sample calculation of the stiffness is provided below.

$$\text{Stiffness, } K = \Delta F / \Delta l$$

where, ΔF = change in the load

Δl = change in the displacement

$$K = \frac{(287.58 - 215.17)\text{kN}}{(0.02246 - 0.02036)\text{m}}$$

$$K = 34480.1 \text{ kN/m}$$

The variation of the vertical stiffness with shape factor is plotted as shown in the Figure 5.2. It shows that with the increase in shape factor the vertical stiffness is found to increase.

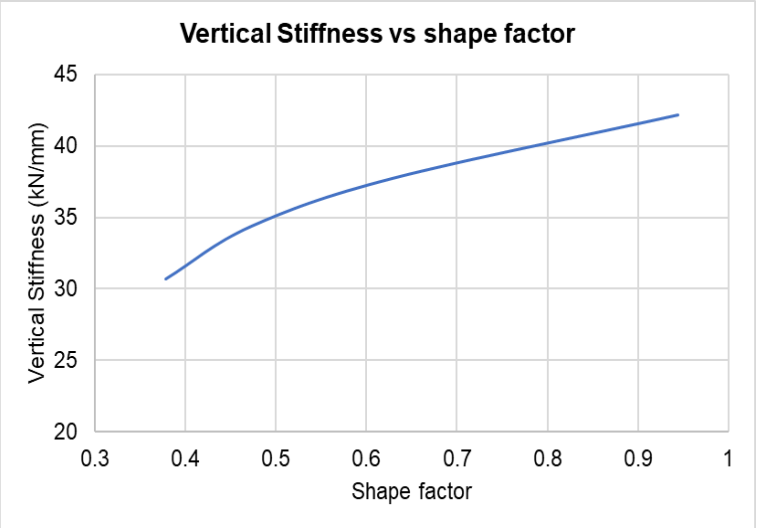

Figure 5.2 Vertical stiffness vs shape factor

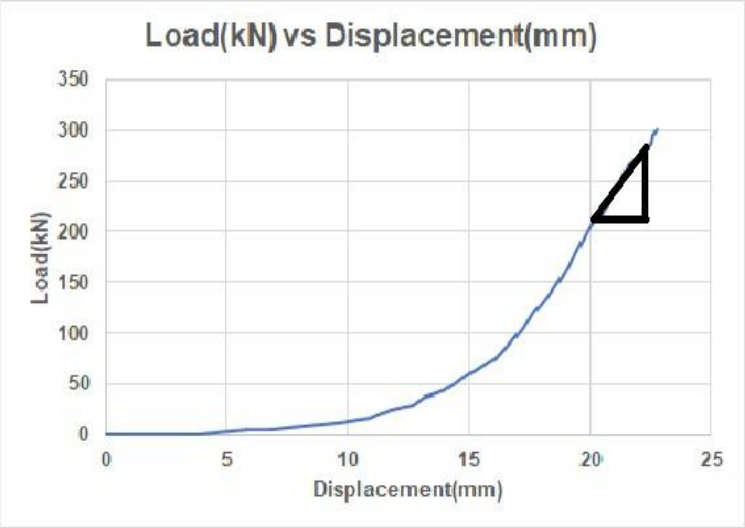

Figure 5.3. Load (kN) vs displacement(mm) plot for stiffness evaluation

The stiffness is calculated from the slope and the variation of vertical stiffness with respect to change in shape factor is obtained as provided in the Table 5-1. The shape factor of the given base isolator can be defined as the top area of the isolator divided by free to bulge area. The variation of vertical stiffness is graphically provided as shown in the Figure 5.2

5.2.3 Effect of the Number of Layers on Compressive Strength

The isolator properties depend on the height of the isolator which is a function of shape factor. Hence to study whether the shape factor has an effect on the variation of compressive strength, analysis is conducted. The load at which the breakage is observed is taken as the load for the calculation of compressive strength. The variation of compressive strength with respect to increase is plotted as shown in Figure 5.4. From the graph it can be observed that with respect to increase in shape factor the compressive strength is also increasing but the variation is negligibly small.

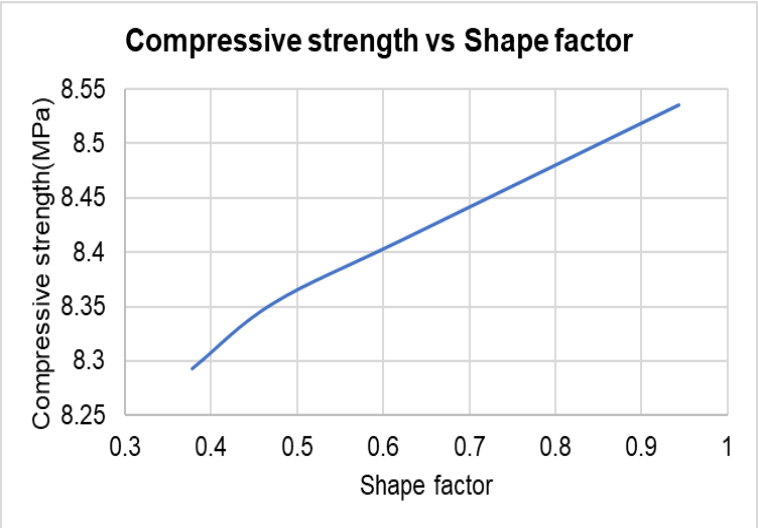

Figure 5.4. Compressive strength vs shape factor

5.3 Cyclic Load Test

The base isolator should have a good level of horizontal flexibility to safeguard the structure above it from seismic damage. The cyclic shear test estimates the horizontal stiffness and damping characteristic of the CSTP isolator specimen. Figure 5.5 to 5.16 shows the representation of the hysteresis loop obtained from the cyclic shear test of different samples.

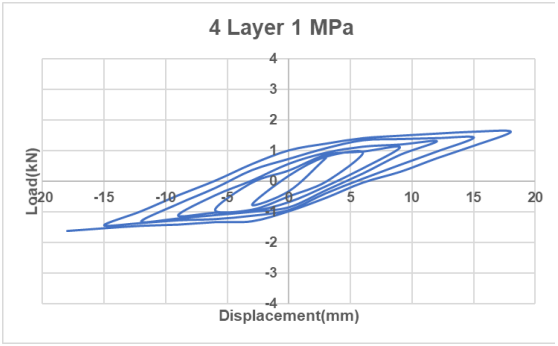

Figure 5.5: 4 Layer 1 MPa hysteresis loop

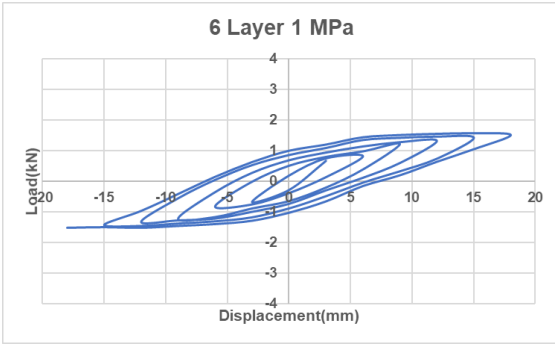

Figure 5.6: 6 Layer 1 MPa hysteresis loop

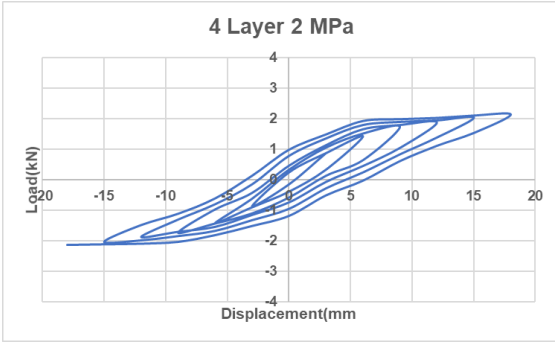

Figure 5.7: 4 Layer 2 MPa hysteresis loop

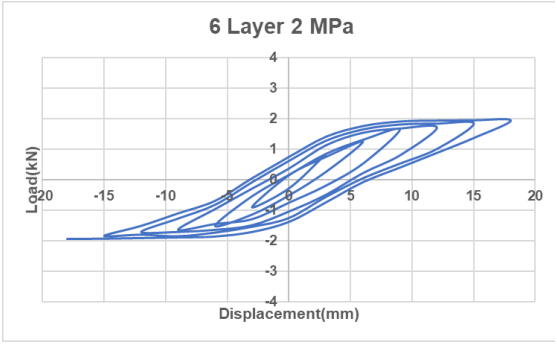

Figure 5.8: 6 Layer 2 MPa hysteresis loop

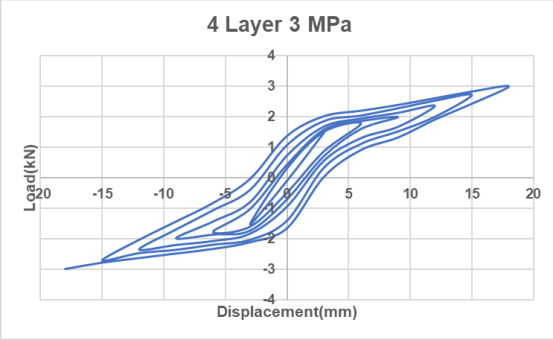

Figure 5.9: 4 Layer 3 MPa hysteresis loop

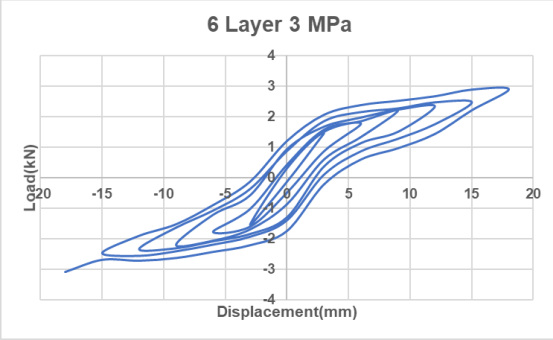

Figure 5.10: 6 Layer 3 MPa hysteresis loop

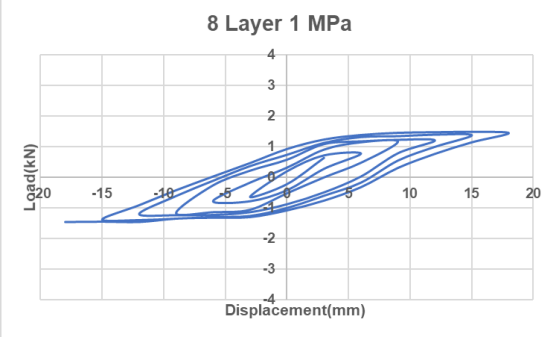

Figure 5.11: 8 Layer 1 MPa hysteresis loop

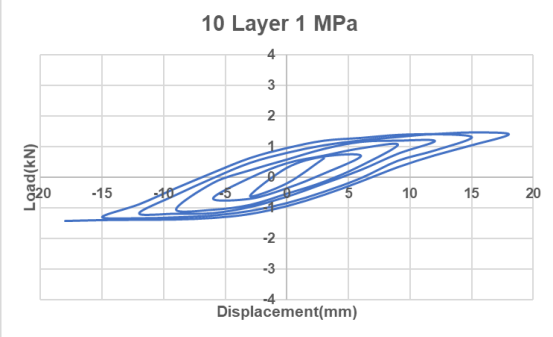

Figure 5.12: 10 Layer 1 MPa hysteresis loop

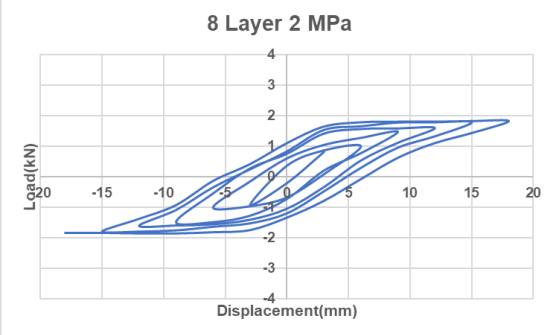

Figure 5.13: 8 Layer 2 MPa hysteresis loop

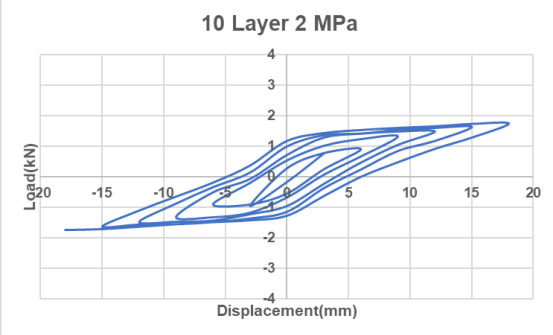

Figure 5.14: 10 Layer 2 MPa hysteresis loop

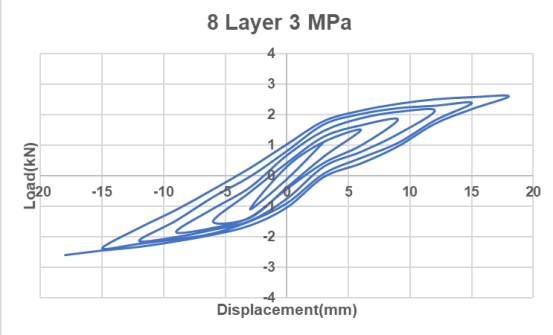

Figure 5.15: 8 Layer 3 MPa hysteresis loop

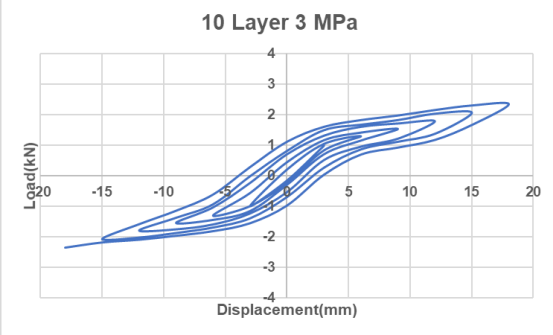

Figure 5.16: 10 Layer 3 MPa hysteresis loop

5.3.1 Horizontal Stiffness of CSTP Isolator

The horizontal stiffness is a very important parameter in the design of the CSTP isolator as it influences the effectiveness of the base isolation capability of the damper. It can be obtained by taking the slope of the hysteresis loop from the cyclic load test (Figure 5.5) The stiffness seems to decrease in each cycle of loading, so the effective horizontal stiffness can be taken corresponding to the outer loop. The isolator's effective horizontal stiffness corresponding to each load cycle of the test can be calculated based on the peak lateral loads and the peak lateral displacements as follows

$$Keff = \frac{Fmax - Fmin}{\Delta max - \Delta min} \qquad \text{(Basar et al.,2021)}$$

where, Keff =Horizontal stiffness of STP isolator

Fmax= peak value of positive horizontal load

Fmin= peak value of negative horizontal load

Δmax= peak value of positive horizontal displacement

Δmin= peak value of negative horizontal displacement

Δmin= peak value of negative horizontal displacement

The horizontal stiffness of the CSTP isolator with a change in shape factor is tabulated in Table 5.1 and is graphically represented as shown in Figure 5.17.

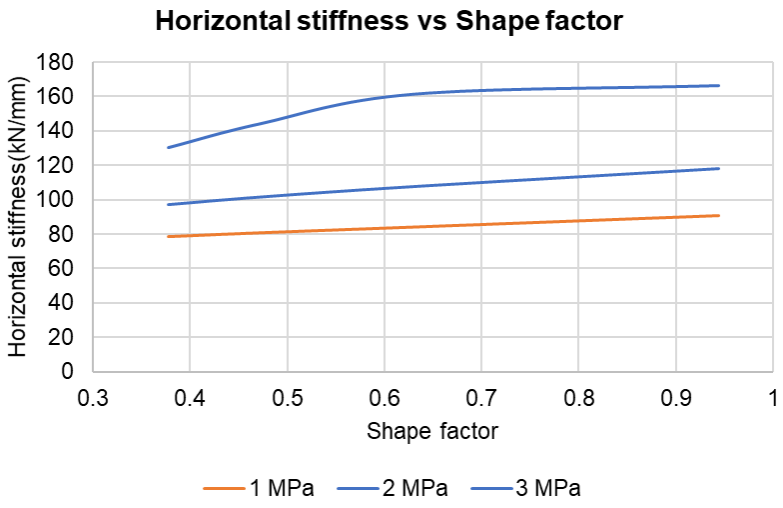

Figure 5.17 Horizontal stiffness vs shape factor

5.3.2 Effective Damping in CSTP Isolator

The effective damping is a measure of the energy absorption capacity of the CSTP isolator, which can be measured by taking the area of the hysteresis loop obtained from the cyclic shear test. The change in damping factor with respect to the change in shape factor is plotted in Figure 5.18. The effective damping (β_{eff}) of an isolator shall be calculated for each cycle of loading by the formula

$$\beta_{eff} = \frac{\left(\frac{2}{\Pi}\right) * Eloop}{(|\Delta^{+}| - |\Delta^{-}|)^{2} * Keff}$$

(Basar et al.,2021)

β_{eff}= Effective damping

E loop= Energy dissipated per cycle of the loading

K_{eff} =Horizontal stiffness of STP isolator

Δ^{+}= peak value of positive horizontal displacement

Δ^{-}= peak value of negative horizontal displacement

Table 5.1 Relationship between shape factor, vertical pressure, effective stiffness and damping factor

Shape factor	1 MPa		2 MPa		3 MPa	
	Effective Stiffness, Keff (kN/mm)	Damping ratio	Effective Stiffness, Keff (kN/mm)	Damping ratio	Effective Stiffness, Keff (kN/mm)	Damping ratio
0.944	90.56	0.204	118.33	0.163	166.67	0.119
0.6293	83.89	0.227	107.78	0.183	161.67	0.134
0.472	80.56	0.229	101.67	0.196	144.44	0.138
0.3776	78.33	0.233	97.22	0.199	130.56	0.141

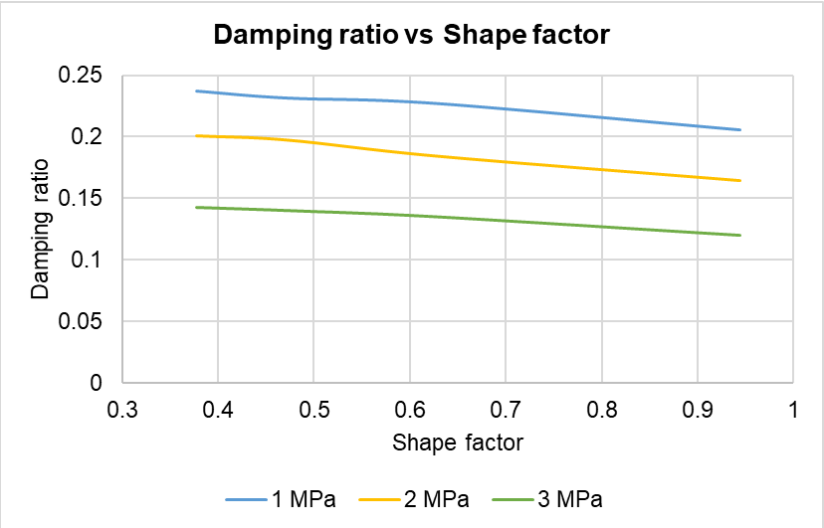

Figure 5.18. Damping ratio vs shape factor

5.3.3 Relation between damping ratio and effective stiffness in CSTP isolator

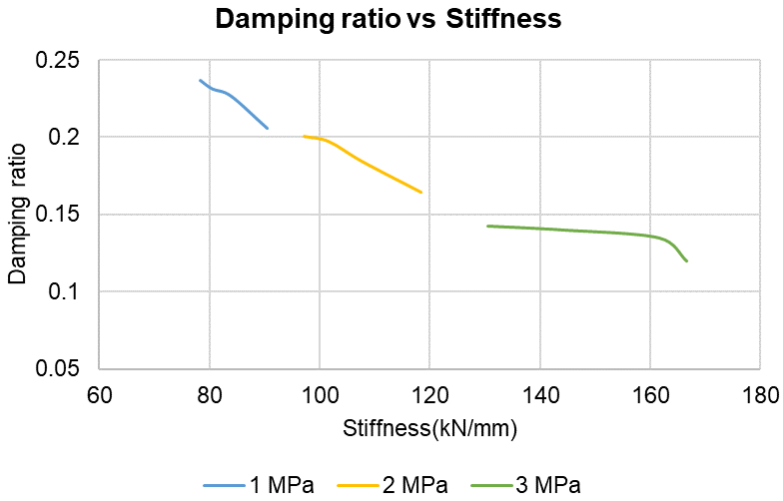

Figure 5.19. Damping ratio vs stiffness

The variation of damping ratio with respect to change in stiffness is plotted in the Figure 5.19. It shows that with the increase in stiffness damping ratio is reducing in all the cases. The maximum decrease in damping ratio is observed in case of 1 MPa and when it comes to the case of 3 MPa the percentage decrease is less as compared to all other cases.

Chapter 6

Validation of the Model

6.1. General

The validation of the model is done with reference to Basar et al., 2021. The dimensions of the masonry model and the material properties are as discussed in the Table 6.1 and Table 6.2 respectively.

Table 6.1 Geometric properties of the model

Length (m)	7.5m
Width (m)	5.5m
Story height (m)	3m
Thickness of the slab (m)	0.40m
Dimension of the basement beam (m x m)	0.625x0.750m

Table 6.2 Material properties of the model

Unit weight of the brick masonry	18500 N/mm
Masonry compressive strength	6MPa
Modulus of elasticity of material	3300000MPa
Grade of concrete	M25
Grade of steel	Fe 415

The Figure 6.1 shows the plan, elevation, three-dimensional model and the corresponding stress distribution of the model in response to El Centro earthquake.

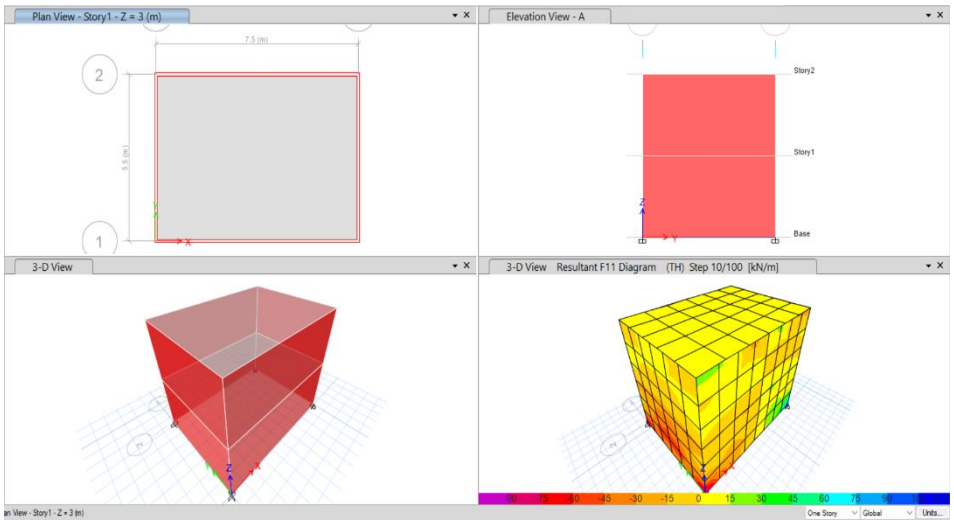

Figure 6.1 Validation model

6.2. Comparison of the Result

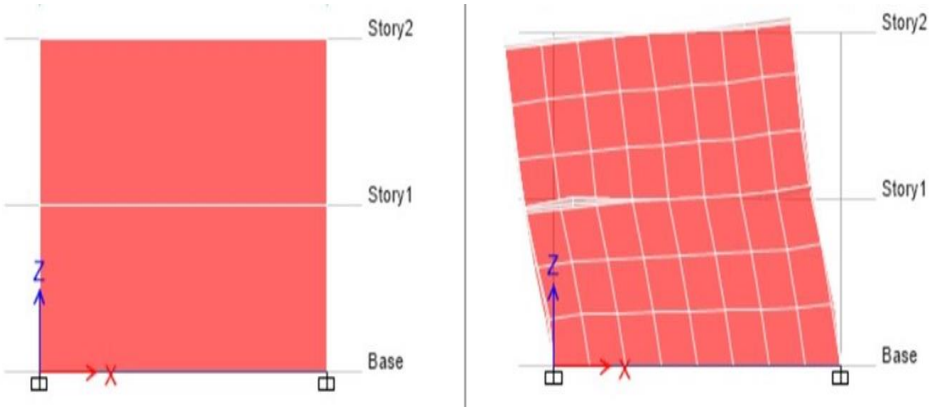

Figure 6.2 Response of the fixed model

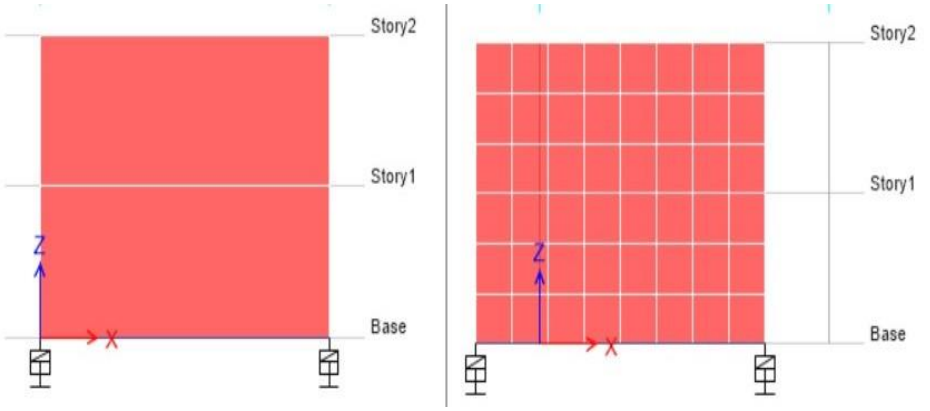

Figure 6.3 Response of the base isolated model

The response of the structure with and without the isolator is analysed and is compared with the reference value. Figure 6.2 shows the performance of the structure without being isolated and Figure 6.3 show the performance which is isolated with the isolator. The model which is not base isolated undergoes structural deformations which induce stresses in the structure and when it is isolated the base isolator undergoes deformations and it absorbs the energy and due to the corresponding damping action, the structure will be safe from failure.

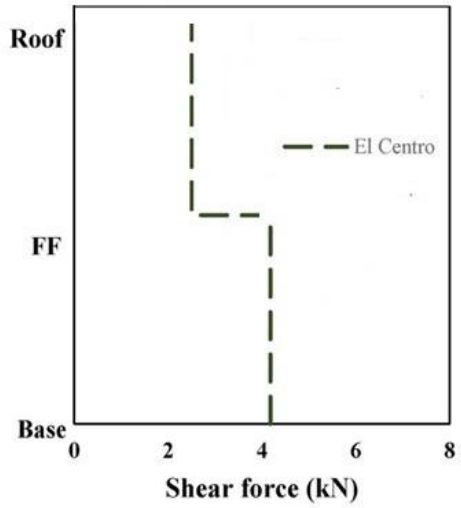

Figure 6.4 Shear force of fixed base form reference value

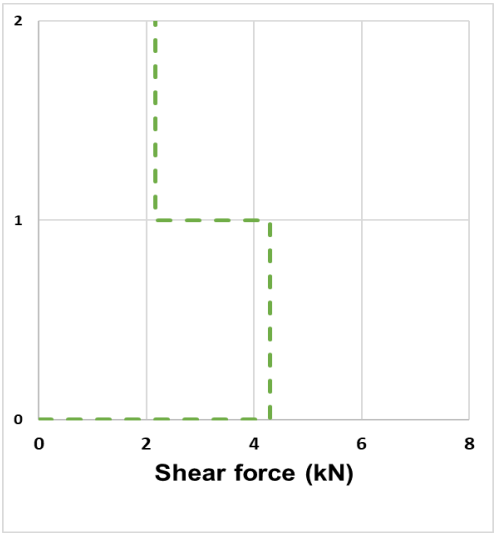

Figure 6.5 Shear force of fixed base form numerical analysis value

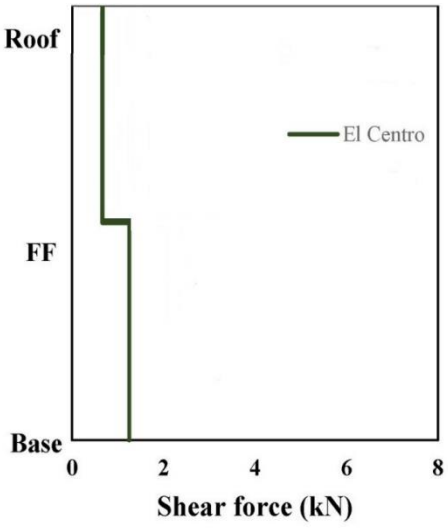

Figure 6.6 Shear force of base isolated model form reference value

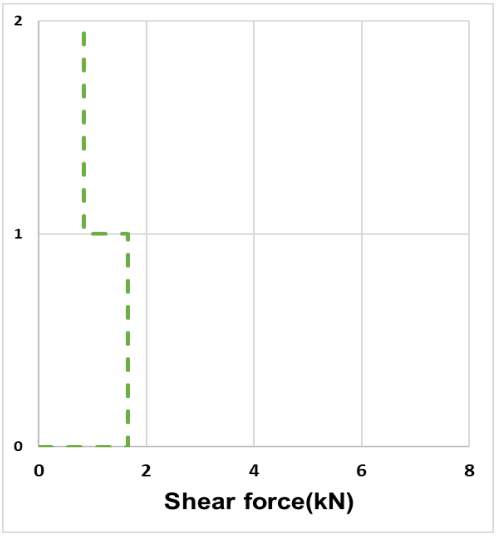

Figure 6.7 Shear force of base isolated model form reference value

The shear force of the reference model without (Figure 6.4 and Figure 6.5) and with base isolator (Figure 6.6 and Figure 6.7) is compared to that obtained from the nonlinear time history analysis from ETABS software and is found to be in close agreement with the reference values

The percentage error in the story shear between the reference model and the validation model is provided in Table 6.3 and Table 6.4, which implies the percentage difference is less than 7 percent and is found to be within the acceptable limit.

Table 6.3 Story shear of plane frame model

Plane frame model	Journal Values	Validation Values	Percentage Error
Base	4.10	4.292	4.68
Story 1	2.3	2.22	4.34
Story 2	2.3	2.22	4.34

Table 6.4 Story shear of base isolated model

Base isolated model	Journal Values	Validation Values	Percentage Error
Base	1.75	1.662	5.03
Story 1	0.9	0.839	6.77
Story 2	0.9	0.839	6.77

Chapter 7

Numerical Analysis of Masonry Structure

7.1 General

The numerical analysis is conducted in the ETABS software package to analyse the performance of the different damper sets subjected to earthquake ground motion. As discussed in the methodology, the primary objective of numerical analysis is to acquire the required amount of data to train the Machine Learning models. Non-linear time history analysis is conducted on unreinforced masonry structures with the El Centro earthquake as the input ground motion. The geometric details of the model are provided in Table 7.1, and the material properties adapted are discussed in Table 7.2.

Table 7.1 Geometric details of the model

Depth of the plinth beam	500mm
Width of the plinth beam	300mm
Thickness of the slab	150mm
Thickness of masonry wall	230mm

Table 7.2 Material properties of the model

Unit weight of the brick masonry	18500 N/mm
Masonry compressive strength	6MPa
Modulus of elasticity of material	3300000MPa
Grade of concrete	M25
Grade of steel	Fe 415

For the analysis, the structures modelled are symmetrical shapes whose dimensions vary from 3m to 10m. The number of stories considered are one story, two story and three-

story. The material properties are adopted from the reference journal Basar et al., 2021. The input ground motion selected is El Centro earthquake of 2021. The response spectra of the earthquake motion is provided in Figure 7.1.

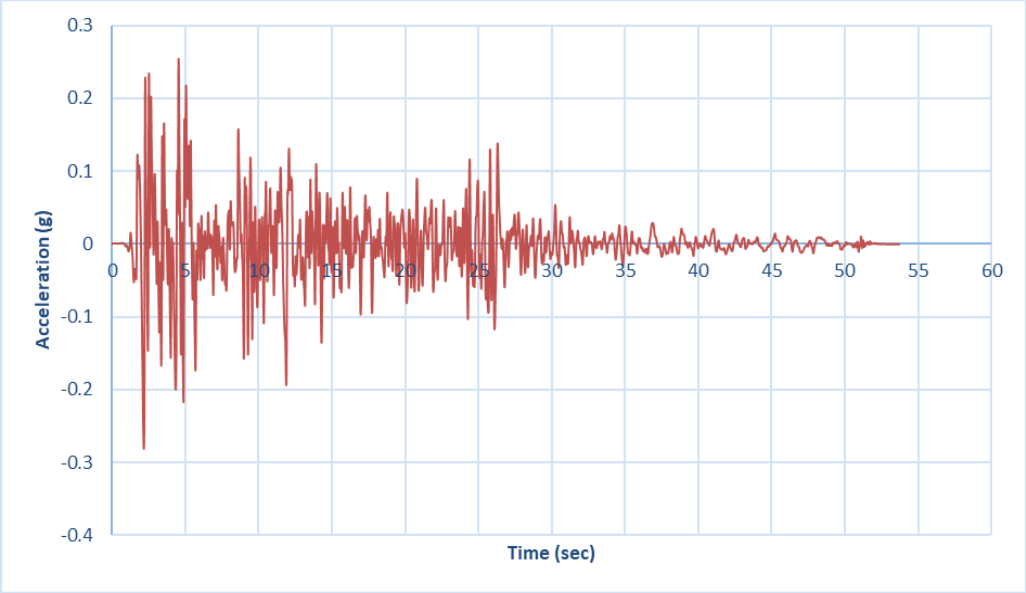

Figure 7.1 El Centro earthquake of 2021

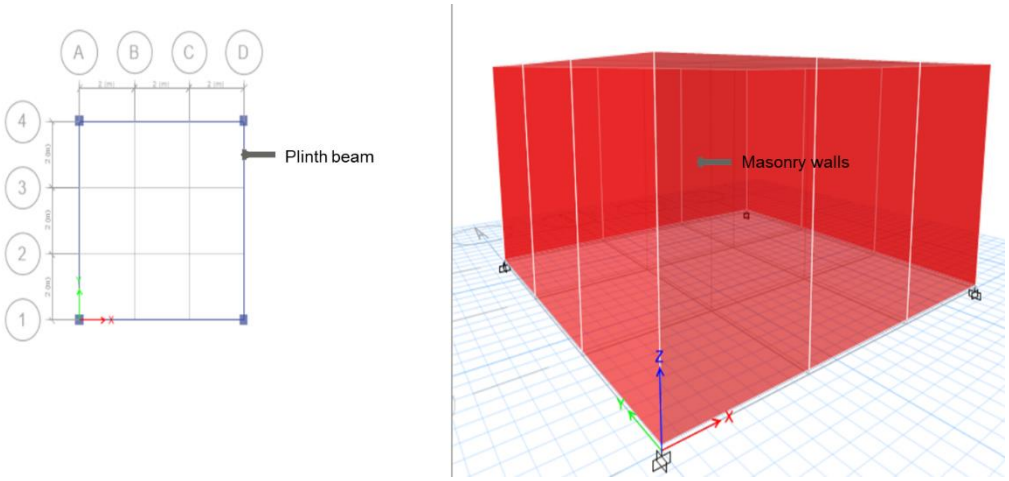

Figure 7.2 A model for numerical analysis

7.2 Damper Data

The damper data for modeling is adopted from the compression and cyclic load test results discussed in section 5. The consolidated data which is used as input for damper properties in ETABS are as provided in Table 7.3. The dampers are classified into 12 different dampers based on the vertical stress applied and the corresponding shear behaviour.

Table 7.3 Details of the damper used in the study

Name	Shape Factor	Vertical Pressure (MPa)	Vertical Load, VL (kN)	Damping ratio	Horizontal Stiffness, KH (kN/mm)
A1	0.944	1	66.052	0.204	90.56
A2	0.944	2	132.103	0.163	118.33
A3	0.944	3	198.155	0.119	166.67
B1	0.6293	1	66.052	0.227	83.89
B2	0.6293	2	132.103	0.183	107.78
B3	0.6293	3	198.155	0.134	161.67
C1	0.472	1	66.052	0.229	80.56
C2	0.472	2	132.103	0.196	101.67
C3	0.472	3	198.155	0.138	144.44
D1	0.3776	1	66.052	0.233	78.33
D2	0.3776	2	132.103	0.199	97.22
D3	0.3776	3	198.155	0.141	130.56

7.3 Nomenclature of Dampers

The first letter of the dampers specifies the shape factor of the damper as shown in Table 7.4. The dampers are named from A to D representing the corresponding variation of the shape factor from 0.944 to 0.3776. The numerical value represents the vertical pressure for which the damper is tested/ as designed as shown in Table 7.5.

Table 7.4 Nomenclature of damper based on shape factor

Terminology	Shape Factor
A	0.944
B	0.6293
C	0.472
D	0.3776

Table 7.5 Nomenclature of dampers based on vertical pressure

Terminology	Vertical pressure (MPa)
1	1 MPa
2	2 MPa
3	3 MPa

7.4 Placement of Dampers on the Building

The dampers are proposed to be placed under the plinth beam. As the presented study is focused on masonry structures, it is reasonable to assume that the load will be uniformly distributed under the plinth beam. The dampers which are placed should satisfy two criteria. The first is that it should be able to transfer the vertical load of the building, and secondly, it must provide the desired horizontal stiffness. The higher horizontal stiffness makes the system behave rigidly, and too low horizontal stiffness creates a longer time period, hence it doesn't serve the desired purpose. In addition, the number of dampers units should be selected based on the configuration of the building.

The procedure adopted in the study for the selection of the optimum number of samples is to first fix the target time period of the building. After fixing the target time period, the required stiffness is calculated based on the mass of the building and the target time period. The stiffness required is then divided by the individual stiffness of the damper units with respect to the shape factor as provided in Table 7.3 to get the number of damper units required. Also, before finalizing the number, it should be made sure that the dampers are able to meet the vertical load transfer criteria. If the number of damper units obtained from the required stiffness criteria doesn't meet the vertical load transfer criteria, suitable variations in the number can be made to satisfy the vertical load transfer criteria. The dampers are proposed to be placed below the plinth beam such that the load from the superstructure will be transferred through the plinth beam and then through the dampers to reach the foundation. Under the action of earthquake loading, the superstructure is expected to act as an individual unit such that deformations are possible only at the base isolator level. The spacing of the dampers will be decided based on the number of units of the isolator required and the dimensions of the building.

An example of the placement of the isolator from the ETABS interface is depicted in Figure 7.3. The plan view of the 5m x 5m model with 1 MPa, 2 MPa, and 3 MPa damper combinations is represented in Figure 7.3, Figure 7.4 and Figure 7.5 and its corresponding 3D model is represented in Figure 7.6, Figure 7.7 and Figure 7.8 respectively.

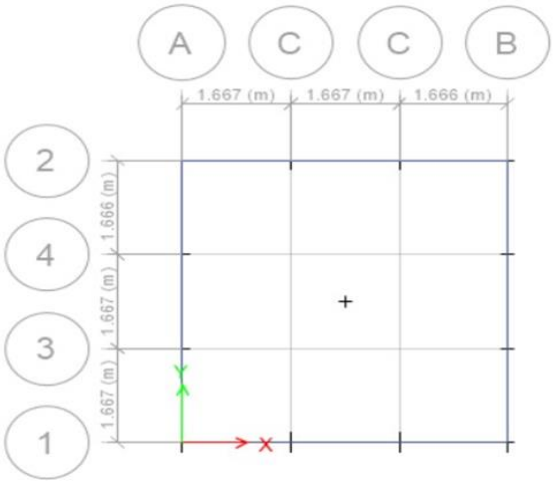

Figure 7.3 Plan layout for 5m x 5m model with 1 MPa damper

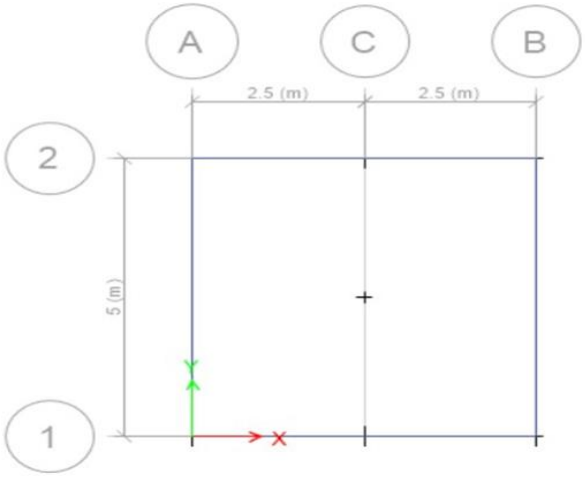

Figure 7.4 Plan layout for 5m x 5m model with 2 MPa damper

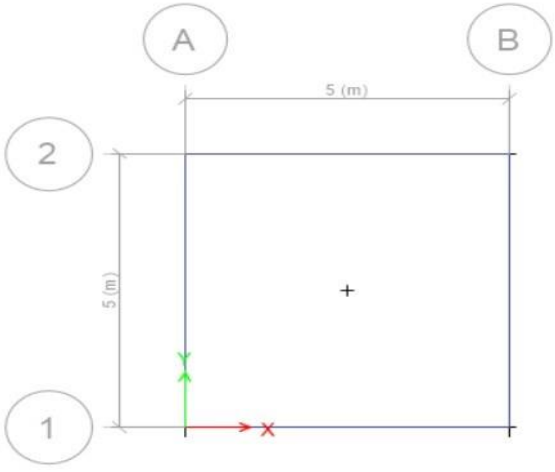

Figure 7.5 Plan layout for 5m x 5m model with 3 MPa damper

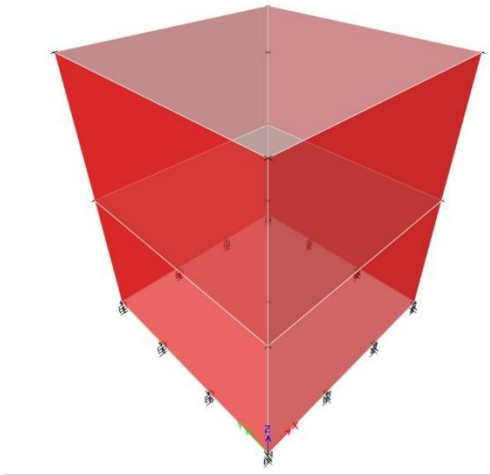

Figure 7.6 3D model for 2 story (5m x 5m) with 1 MPa damper

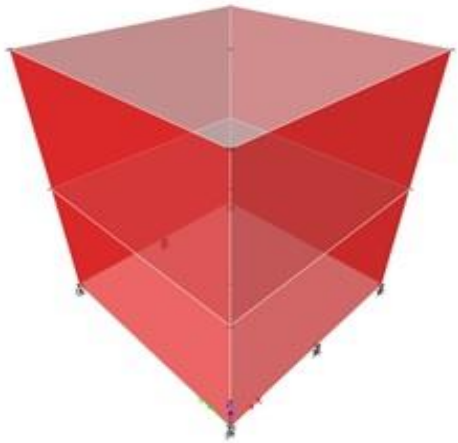

Figure 7.7 3D model for 2 story (5m x 5m) with 2 MPa damper

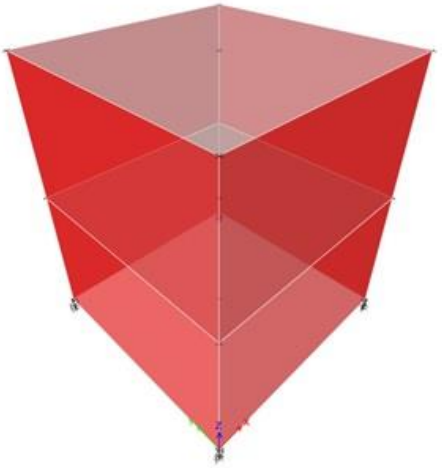

Figure 7.8 3D model for 2 story (5m x 5m) with 3 MPa damper

7.5 Generation of the Dataset

As explained in section 7.1 the models for the analysis are created in the ETABS model. For each of variation in the dimension and number of stories, the performance of 12 available dampers is analysed. A total of 312 models including 288 models with base isolation and 24 plane frame models were modelled. The properties of the damper in relation to shape factor is listed in the Table 7.3. The base shear, spacing in the x and y direction, number of units required for the isolation and its time period are also noted. For each combination of length, breadth and number of stories the dampers combination is ranked based on the shift in base shear. The mass of the building can be calculated from ETABS and the target time period is fixed as 2.5s from which the required stiffness be can calculated. Hence by using the value of this required stiffness the achievable stiffness by using the damper units is calculated and is used to find the corresponding results. The summary of the data is tabulated in a excel sheet to train the Machine Learning (ML) models as depicted in Figure 7.9.

The first 3 columns represent the building parameters: length, breadth, and the number of stories, the KH represents the horizontal stiffness of the individual damper, Ke represents the effective stiffness of the damper combination, VL represents the load capacity of the damper, VL/KH is the ratio of the vertical load capacity to the horizontal stiffness of the individual damper, and the next column represents the name of the damper used. The following columns represent the units, rankings, base shear, time period, spacing in the x and y directions, and change in base shear respectively.

7.6 Results and Discussion on Numerical Analysis

From the numerical analysis conducted on the masonry structure using the 12 sets of isolators the required data for the machine learning modelling is generated. The figure 7.10 shows a summary of the performance of 12 different sets of isolators. It represents the minimum and maximum change in base shear observed from each type of isolator used The black coloured bar represents the minimum observed change in base shear and the yellow bar represents the maximum observed change in base shear for a specific isolator set.

.

length	breadth	No of stories	KH	Ke	VL	VL/KH	Damper	Units	Rankings	BS0	Tp	SX	SY	Change in BS0
3	3	1	166.667	666.667	198.155	1.18893	A3	4	12	0.596	1.2023	0	0	37.38
3	3	1	161.667	646.668	198.155	1.2257	B3	4	11	0.5874	1.2208	0	0	38.29
3	3	1	144.444	577.778	198.155	1.37184	C3	4	10	0.5547	1.2915	0	0	41.72
3	3	1	130.556	522.222	198.155	1.51778	D3	4	9	0.522	1.358	0	0	45.16
3	3	1	118.333	473.333	132.103	1.11636	A2	4	8	0.4862	1.426	0	0	48.92
3	3	1	107.778	431.111	132.103	1.2257	B2	4	7	0.456	1.495	0	0	52.09
3	3	1	101.667	406.667	132.103	1.29937	C2	4	6	0.438	1.539	0	0	53.98
3	3	1	97.2222	388.889	132.103	1.35877	D2	4	5	0.426	1.5742	0	0	55.24
3	3	1	90.5556	362.222	66.052	0.72941	A1	4	4	0.4024	1.6312	0	0	57.72
3	3	1	83.8889	335.556	66.052	0.78737	B1	4	3	0.3792	1.6948	0	0	60.16
3	3	1	80.5556	322.222	66.052	0.81996	C1	4	2	0.3675	1.729	0	0	61.39
3	3	1	78.33	313.32	66.052	0.84325	D1	4	1	0.3602	1.7538	0	0	62.16
4	4	1	166.667	666.667	198.155	1.18893	A3	4	12	0.718	1.42	0	0	48.64
4	4	1	161.667	646.668	198.155	1.2257	B3	4	11	0.7038	1.4423	0	0	49.66
4	4	1	144.444	577.778	198.155	1.37184	C3	4	10	0.6532	1.5259	0	0	53.28
4	4	1	90.5556	543.333	66.052	0.72941	A1	6	9	0.6247	1.5736	2	0	55.31
4	4	1	130.556	522.222	198.155	1.51778	D3	4	8	0.6067	1.605	0	0	56.6
4	4	1	83.8889	503.333	66.052	0.78737	B1	6	7	0.5898	1.635	2	0	57.81
4	4	1	80.5556	483.333	66.052	0.81996	C1	6	6	0.5718	1.6684	2	0	59.1
4	4	1	78.33	469.98	66.052	0.84325	D1	6	5	0.5609	1.6919	2	0	59.88
4	4	1	118.333	473.333	132.103	1.11636	A2	4	4	0.5568	1.6859	0	0	60.17
4	4	1	107.778	431.111	132.103	1.2257	B2	4	3	0.5179	1.7665	0	0	62.95
4	4	1	101.667	406.667	132.103	1.29937	C2	4	2	0.4944	1.818	0	0	64.64
4	4	1	97.2222	388.889	132.103	1.35877	D2	4	1	0.4793	1.86	0	0	65.72
5	5	1	90.5556	724.444	66.052	0.72941	A1	8	12	0.8665	1.557	2.5	2.5	54.63
5	5	1	83.8889	671.111	66.052	0.78737	B1	8	11	0.8184	1.618	2.5	2.5	57.15
5	5	1	166.667	666.667	198.155	1.18893	A3	4	10	0.80604	1.6235	0	0	57.79
5	5	1	80.5556	644.444	66.052	0.81996	C1	8	9	0.7937	1.6513	2.5	2.5	58.44
5	5	1	161.667	646.668	198.155	1.2257	B3	4	8	0.7879	1.648	0	0	58.74
5	5	1	78.33	626.64	66.052	0.84325	D1	8	7	0.7786	1.6745	2.5	2.5	59.23
5	5	1	144.444	577.778	198.155	1.37184	C3	4	6	0.7248	1.7439	0	0	62.05
5	5	1	130.556	522.222	198.155	1.51778	D3	4	5	0.6682	1.8343	0	0	65.01

Figure 7.9 Data obtained from the numerical analysis

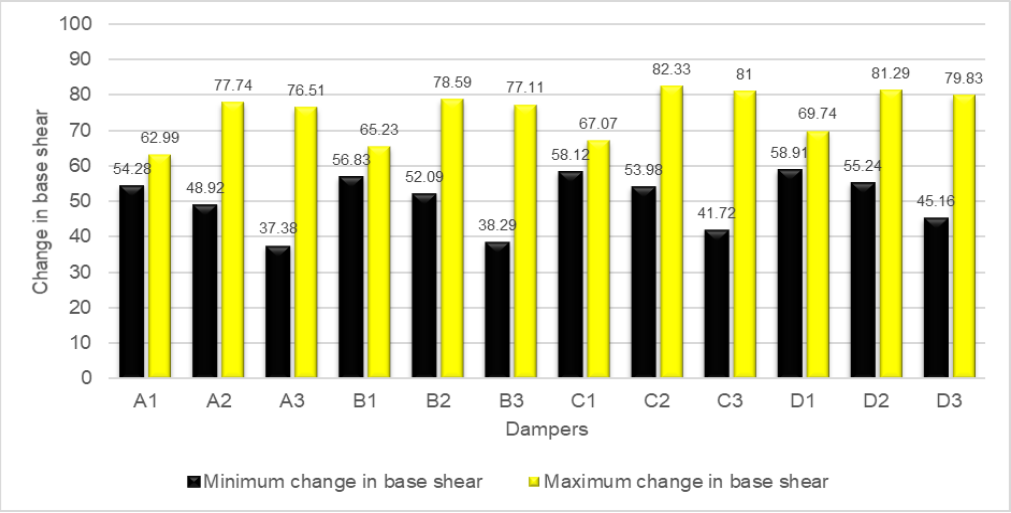

Figure 7.10 Performance analysis of the dampers

From Figure 7.10 it can be inferred that the performance of the isolator does not only depend on the damper properties but also on the characteristic of the building. Hence it shows the significance of the optimum design of the isolator layout for the building. It can be observed that by choosing the optimum design base shear can be reduced up to 80 percent

Chapter 8

Machine Learning Model

8.1 General

Machine Learning is a subfield of artificial intelligence that is gaining prominence in all fields. Models based on Machine Learning can be conceptualized as a program that has been trained to identify patterns in new data and make predictions. These models are represented as a mathematical function that accepts requests in the form of input data, and returns an output in response. By utilizing a set of training data, these algorithms themselves find various patterns and recognize the correlation between the input parameters in order to make predictions on the unseen data. It is possible to effectively analyse data using ML algorithms, which can perform operations such as classification, regression, etc. Various algorithms are available for building machine learning models the choice of a particular model depends on the accuracy and reliability of the results. Some of the available machine learning packages include linear regression, support vector machines, Naive Bayes, decision trees, random forests, neural networks, gradient boosting, etc. Machine Learning models can be used in the field of earthquake engineering and base isolation systems. The ML models are used to find the peak displacements of the base isolation system in the studies by D. Nguyen et al.,2021 and by D. Nguyen et al.,2022.

In the present study, the ML models used are

i. Artificial Neural Network (ANN)
ii. Random Forest (RF)
iii. Extreme Gradient Boosting (XG Boost)

8.1 Artificial Neural Network

An artificial neural network (ANN) is a computational model that consists of several processing elements that receive inputs and deliver outputs based on their predefined activation functions. Specific architecture format, which is inspired by a biological nervous system. Similar to the structure of the human brain, the ANN models consist of neurons in a complex and nonlinear form

8.1.2 Architecture of ANN

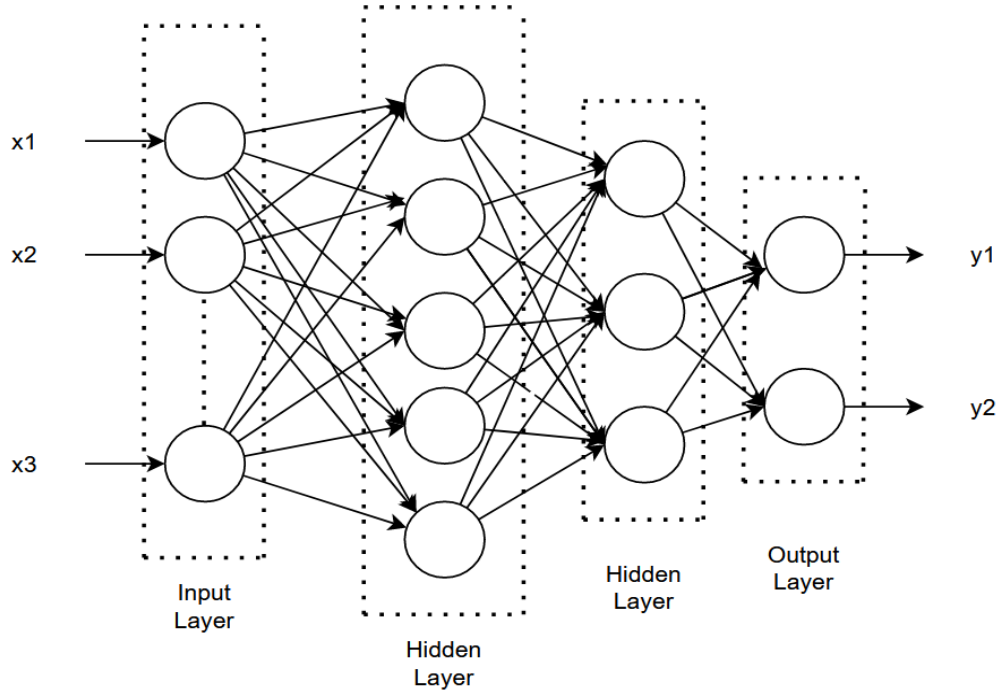

Figure 8.1 Architecture of ANN

An artificial neural network (ANN) is a computational model that consists of several processing elements that receive inputs and deliver outputs based on their predefined activation functions. Specific architecture format, which is inspired by a biological nervous system. Similar to the structure of the human brain, the ANN models consist of neurons in a complex and nonlinear form. Neurons are connected to each other by weighted links. It consists of an input layer that receives the input parameter and passes through hidden layers to reach the output layer. The neurons on each layer are interconnected by means of connecting systems called channels. The channels are designated with certain numerical values called weights that are multiplied by the output from the input layer to act as the input for the hidden layer. The neurons in the hidden

layer contain another numeric value known as bias. The bias value is also applied to the weighted value and it is compared with a threshold function called the activation function which determines the neurons on hidden layers are activated or not and this process continues till it reaches the output layer. The basic architecture of ANN is shown in Figure 8.1.

8.2 Random Forest

Random Forest (RF) makes use of ensemble learning, a method for solving complex problems by combining a number of classifiers. Due to its precision, ease of use, and adaptability, it serves as one of the most widely used algorithms. A collection of decision trees makes up the "forest" it creates. A forest of decision trees is created. To ensure the most precise predictions, information from the individual trees is then combined.

8.2.1 Architecture of ANN

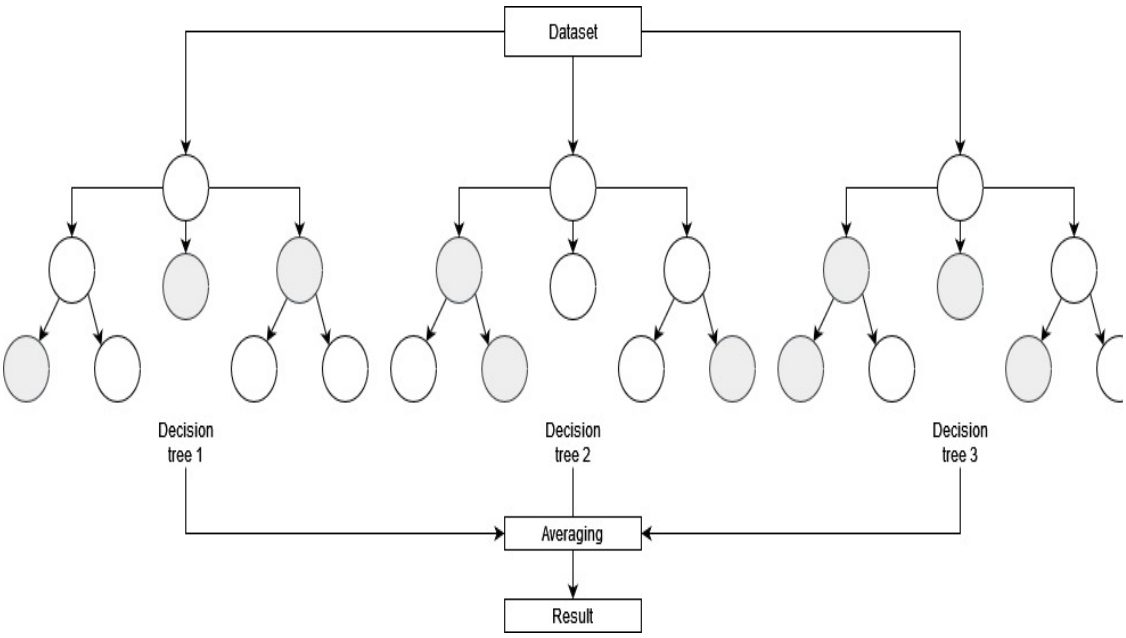

Figure 8.2 Architecture of ANN

The RF model consists of a number of individual trees. The dataset is allowed to pass through the individual trees. Each of the individual trees predict the output independently The results from each of the tree were averaged to obtain the final result. The basic architecture of RF model is shown in Figure 8.2.

8.3 Extreme Gradient Boosting (XG Boost)

Extreme Gradient Boosting which is also called XG Boost is a gradient boosting algorithm that predicts the output from a group of decision trees. This algorithm is known for its high accuracy and speed of prediction. It is been widely employed in data science and has excelled in a number of machine learning challenges.

8.3.1 Architecture of XG Boost

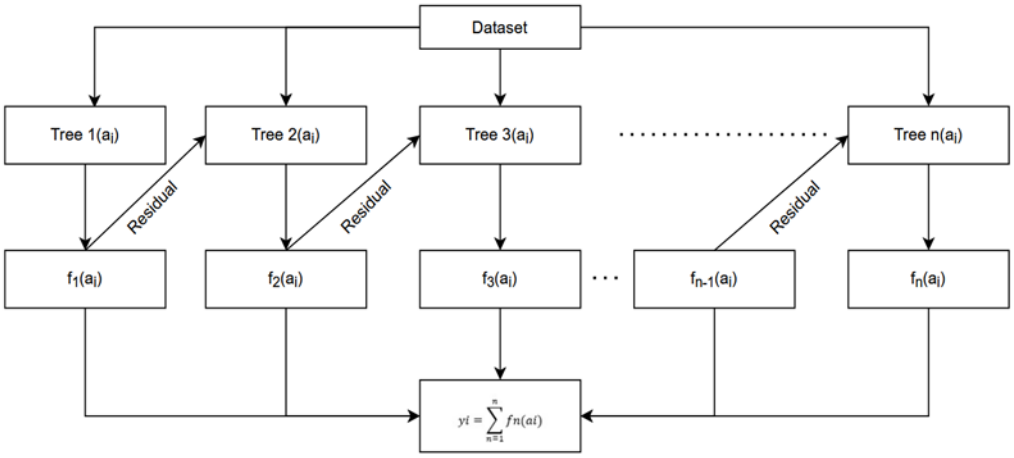

Figure 8.3 Architecture of XG Boost

The XG Boost also contains a number of decision trees. In this procedure, the residual from the previous step is used to update the parameters in the following step. In order to combat overfitting, a regularisation is added to the objective function with a loss function as an improvement over the traditional gradient boosting algorithm. As the residual from the previous tree is passed to the next tree, the new trees can take more efficient decisions and thus more and more refined prediction is possible in the case of the XG Boost algorithm. The architecture of the XG Boost algorithm is shown in Figure 8.3.

8.4. Hyperparameter Optimization in the ML Models

The ML models consist of several hyperparameters that can be tuned to obtain the optimal results. These parameters within the model can be set values prior to the training itself. It is a crucial step in the workflow for machine learning and should be carried out in a systematic manner and with proper consideration to get the best outcomes. Hence hypermeter tuning is done in the study to get the best results.

8.2.1 ANN Model

The ANN architecture employed in the present study has seven layers with varying numbers of units in each layer. The number of units in each layer is 96,48,24,12,6,3 and 1 respectively and is chosen by trial and error method. The activation functions employed in all the hidden layers are rectified linear units (ReLU), which is a common choice for deep learning models due to its ability to handle nonlinearity in data. As it is a regression model no activation function is used in the final layer.

8.2.2 Random Forest Model

A grid search is performed using GridSearchCV() to search for the optimal combination of hyperparameters for the Random Forest regression model. The hyperparameters and their respective values to search over are specified in a dictionary called param_grid_rf. The GridSearchCV () method then fits the Random Forest model to the training data for each combination of hyperparameters in the grid and selects the combination that performs the best based on the specified scoring metric and cross-validation strategy. The hyperparameters used in the study include:

- n_estimators: the number of trees used
- max_depth: the maximum depth of individual trees
- max_features: the maximum number of features to be considered while splitting a node
- min_samples_leaf: the minimum number of expected samples at a leaf node
- bootstrap: whether bootstrap samples are used when building trees

In this study, the mean squared error (MSE) is used as the scoring metric, and a 3-fold cross-validation is used. After the grid search is complete, the best estimator (i.e., the best combination of hyperparameters) is selected and used to make predictions on the test set.

8.2.3 XG Boost Model

The XGBoost model is tuned using Grid Search, which tries different combinations of hyperparameters to find the best-performing one. The hyperparameters that are tuned in this model are:

- max_depth: The maximum depth of the individual tree.
- min_child_weight: The minimum sum of child instance weight
- subsample: The subsample ratio used in training instances.
- colsample_bytree: The subsample ratio of columns while constructing a tree.

- eta: The learning rate.

For each hyperparameter, a list of possible values is defined in XGB_params_grid_. The Grid Search algorithm trains and evaluates the model with all possible combinations of hyperparameters and returns the best-performing model.

Chapter 9

Input Parameters for ML Models

9.1 General

The study involves the prediction of the number of units, spacing in the x and y directions, rank, base shear, and time period of the structure. The predictions are based on the data obtained from the numerical data obtained from nonlinear time history analysis done on the ETABS software package, as mentioned in the section. To improve the accuracy of the output from the ML models, the data from the ETABS has to be pre-processed. This includes adequate standardization and finding the correlation between the input parameters, thus eliminating the unwanted input variables. Hence, to achieve the goal, the dataset mentioned in the section is made into two datasets, as explained in the following sections.

9.1.1 Prediction of Number of Units, Spacing in x Direction, Spacing in y Direction

The building parameters and the damper parameters such as horizontal stiffness of individual damper, vertical load capacity of damper, and L_V/K_H ratio are used for the purpose as shown in Table 9.1. The damper parameters are selected based on the effectiveness of prediction results and the sample data is shown in Figure 9.1.

Table 9.1 Input parameters for the units, spacing in x direction, spacing in y direction

Building parameters	Damper parameters
Length	Horizontal stiffness of individual damper, K_H
Breadth	Vertical load capacity of damper, V_L
Number of stories	V_L/K_H ratio

9.1.2 Prediction of Rank, Base Shear, Time Period

Here in addition to the above-mentioned damper parameters no of units and total effective stiffness were also used as shown in Table 9.2. The excel sheet used for the ML model study is shown in Figure 9.2.

Table 9.2 Input parameters for the rank, base shear, time period

Building parameters	**Damper parameters**
Length	Horizontal stiffness of individual damper, K_H
Breadth	Vertical load capacity of damper, V_L
Number of stories	V_L/K_H ratio
	No of units
	Total effective stiffness

Length	Breadth	No of stories	KH	VL	VL/KH	Damper	Units	SX	SY
3	3	1	166.667	198.155	1.18893	A3	4	0	0
3	3	1	161.667	198.155	1.2257	B3	4	0	0
3	3	1	144.444	198.155	1.37184	C3	4	0	0
3	3	1	130.556	198.155	1.51778	D3	4	0	0
3	3	1	118.333	132.103	1.11636	A2	4	0	0
3	3	1	107.778	132.103	1.2257	B2	4	0	0
3	3	1	101.667	132.103	1.29937	C2	4	0	0
3	3	1	97.2222	132.103	1.35877	D2	4	0	0
3	3	1	90.5556	66.052	0.72941	A1	4	0	0
3	3	1	83.8889	66.052	0.78737	B1	4	0	0
3	3	1	80.5556	66.052	0.81996	C1	4	0	0
3	3	1	78.33	66.052	0.84325	D1	4	0	0
4	4	1	166.667	198.155	1.18893	A3	4	0	0
4	4	1	161.667	198.155	1.2257	B3	4	0	0
4	4	1	144.444	198.155	1.37184	C3	4	0	0
4	4	1	90.5556	66.052	0.72941	A1	6	2	0
4	4	1	130.556	198.155	1.51778	D3	4	0	0
4	4	1	83.8889	66.052	0.78737	B1	6	2	0
4	4	1	80.5556	66.052	0.81996	C1	6	2	0
4	4	1	78.33	66.052	0.84325	D1	6	2	0
4	4	1	118.333	132.103	1.11636	A2	4	0	0
4	4	1	107.778	132.103	1.2257	B2	4	0	0
4	4	1	101.667	132.103	1.29937	C2	4	0	0
4	4	1	97.2222	132.103	1.35877	D2	4	0	0
5	5	1	90.5556	66.052	0.72941	A1	8	2.5	2.5
5	5	1	83.8889	66.052	0.78737	B1	8	2.5	2.5
5	5	1	166.667	198.155	1.18893	A3	4	0	0
5	5	1	80.5556	66.052	0.81996	C1	8	2.5	2.5
5	5	1	161.667	198.155	1.2257	B3	4	0	0
5	5	1	78.33	66.052	0.84325	D1	8	2.5	2.5
5	5	1	144.444	198.155	1.37184	C3	4	0	0
5	5	1	130.556	198.155	1.51778	D3	4	0	0
5	5	1	118.333	132.103	1.11636	A2	4	0	0
5	5	1	107.778	132.103	1.2257	B2	4	0	0

Figure 9.1 Sheet used to train ML model for units, spacing in x direction, spacing in y direction

Length	Breadth	No of stories	KH	LV	LV/KH	Units	Ke	Damper	Rankings	BS0	Tp
3	3	1	166.667	198.155	1.18893	4	666.667	A3	12	0.596	1.2023
3	3	1	161.667	198.155	1.2257	4	646.668	B3	11	0.5874	1.2208
3	3	1	144.444	198.155	1.37184	4	577.778	C3	10	0.5547	1.2915
3	3	1	130.556	198.155	1.51778	4	522.222	D3	9	0.522	1.358
3	3	1	118.333	132.103	1.11636	4	473.333	A2	8	0.4862	1.426
3	3	1	107.778	132.103	1.2257	4	431.111	B2	7	0.456	1.495
3	3	1	101.667	132.103	1.29937	4	406.667	C2	6	0.438	1.539
3	3	1	97.2222	132.103	1.35877	4	388.889	D2	5	0.426	1.5742
3	3	1	90.5556	66.052	0.72941	4	362.222	A1	4	0.4024	1.6312
3	3	1	83.8889	66.052	0.78737	4	335.556	B1	3	0.3792	1.6948
3	3	1	80.5556	66.052	0.81996	4	322.222	C1	2	0.3675	1.729
3	3	1	78.33	66.052	0.84325	4	313.32	D1	1	0.3602	1.7538
4	4	1	166.667	198.155	1.18893	4	666.667	A3	12	0.718	1.42
4	4	1	161.667	198.155	1.2257	4	646.668	B3	11	0.7038	1.4423
4	4	1	144.444	198.155	1.37184	4	577.778	C3	10	0.6532	1.5259
4	4	1	90.5556	66.052	0.72941	6	543.333	A1	9	0.6247	1.5736
4	4	1	130.556	198.155	1.51778	4	522.222	D3	8	0.6067	1.605
4	4	1	83.8889	66.052	0.78737	6	503.333	B1	7	0.5898	1.635
4	4	1	80.5556	66.052	0.81996	6	483.333	C1	6	0.5718	1.6684
4	4	1	78.33	66.052	0.84325	6	469.98	D1	5	0.5609	1.6919
4	4	1	118.333	132.103	1.11636	4	473.333	A2	4	0.5568	1.6859
4	4	1	107.778	132.103	1.2257	4	431.111	B2	3	0.5179	1.7665
4	4	1	101.667	132.103	1.29937	4	406.667	C2	2	0.4944	1.818
4	4	1	97.2222	132.103	1.35877	4	388.889	D2	1	0.4793	1.86
5	5	1	90.5556	66.052	0.72941	8	724.444	A1	12	0.8665	1.557
5	5	1	83.8889	66.052	0.78737	8	671.111	B1	11	0.8184	1.618
5	5	1	166.667	198.155	1.18893	4	666.667	A3	10	0.80604	1.6235
5	5	1	80.5556	66.052	0.81996	8	644.444	C1	9	0.7937	1.6513
5	5	1	161.667	198.155	1.2257	4	646.668	B3	8	0.7879	1.648
5	5	1	78.33	66.052	0.84325	8	626.64	D1	7	0.7786	1.6745
5	5	1	144.444	198.155	1.37184	4	577.778	C3	6	0.7248	1.7439
5	5	1	130.556	198.155	1.51778	4	522.222	D3	5	0.6682	1.8343
5	5	1	118.333	132.103	1.11636	4	473.333	A2	4	0.6087	1.9267
5	5	1	107.778	132.103	1.2257	4	431.111	B2	3	0.5634	2.01889

Figure 9.2 Sheet used to train ML model for rank, base shear, time period

Chapter 10

Feature Importance Study

10.1 General

The feature importance study is conducted to understand the effect of individual parameters on the desired outcome. The accuracy and efficiency of the prediction of any ML model depend on the parameters that are used to train and test the model. Hence, an accurate selection of the parameters is essential. Although the selection of the parameters is an important step, all the parameters used may or may not have the same effect on the result. Thus, the quality of prediction may depend more on certain specific parameters. Feature importance indicates the contribution of each feature to the model's prediction. It determines the degree to which a specific variable is beneficial for the current algorithm and projection. By removing the unwanted features, the speed and performance of the algorithm can also be improved. The feature importance of various parameters affecting the prediction of each of the required outcomes is analysed and is represented in the form of bar chart. The vertical line in the bar chart shows the possible standard deviation/variation in the importance of the parameter in the corresponding output. The solid bar chart represents the mean of the importance value.

10.2 Results and Discussion on Feature Importance Study

The feature importance study for the prediction of number of dampers is shown in Figure 10.1 which implies that the number of stories, length and breadth are predominant factors that influence the result. The three of them are the building parameters. Reason for the behaviour may be due to the fact as number of stories increases, the overall mass of the building increases. Hence the number of dampers required depends on the total load of the superstructure and load carrying capacity of the individual damper. The importance of length and breadth is less than the number of stories as its corresponding influence on the mass of the building is less as compared to the number of stories. The horizontal stiffness is showing less influence is because of the fact in case of scrap tyre pads the vertical pressure is the limiting factor in the number of units prediction, as it has sufficient horizontal flexibility.

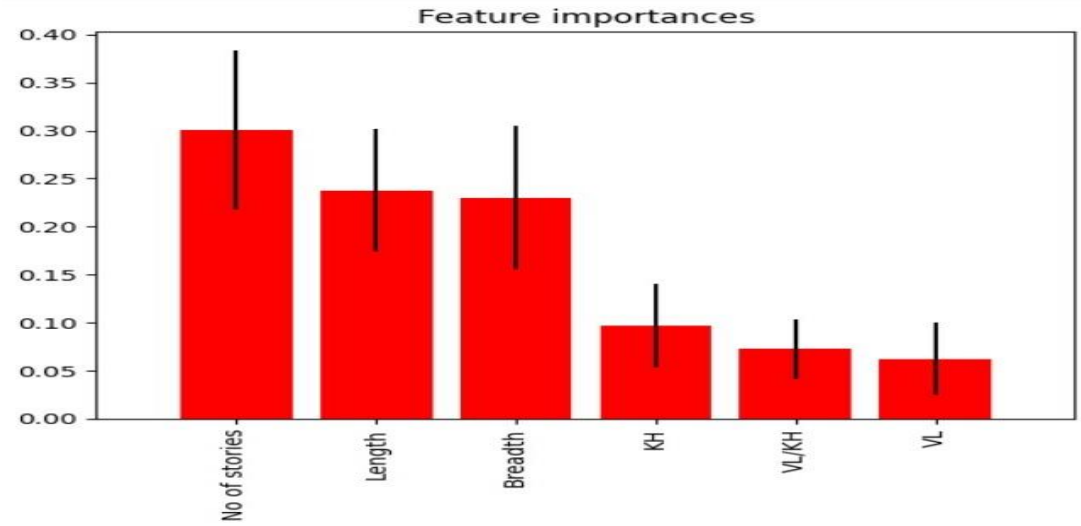

Figure 10.1 Feature importance for the number of units

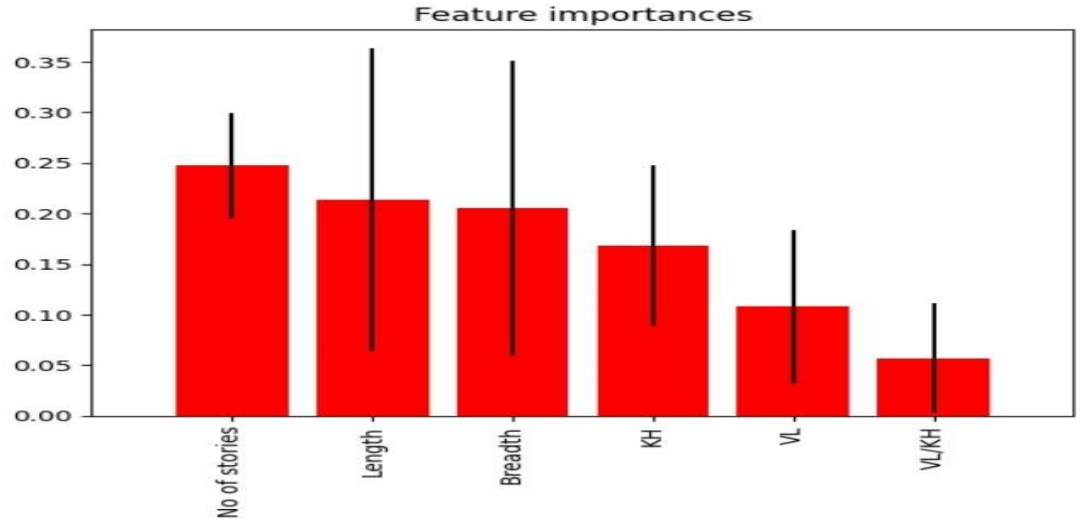

Figure 10.2 Feature importance for spacing in x direction

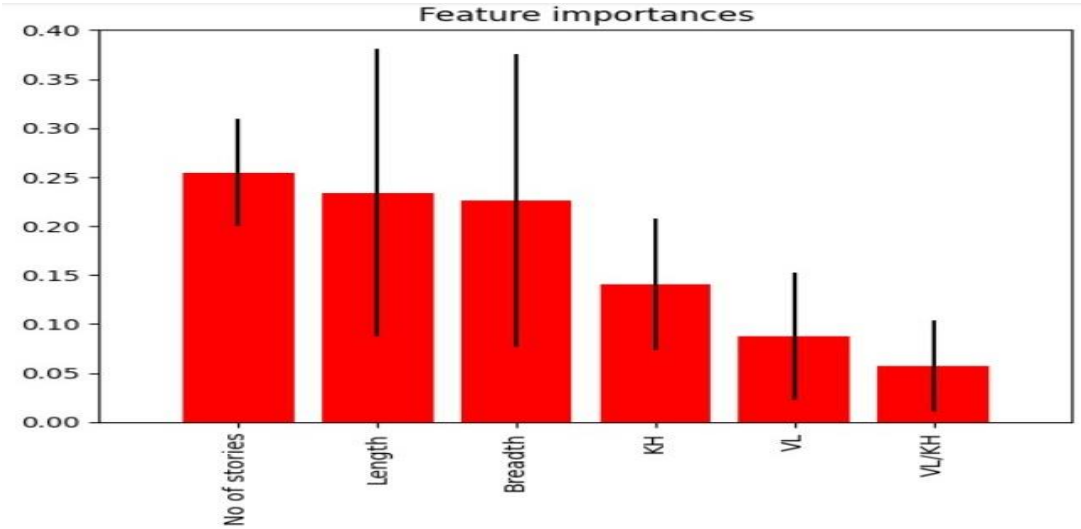

Figure 10.3 Feature importance for the spacing in y direction

Figure 10.2 and 10.3 shows the importance of the input parameters for the prediction of spacing in the x and y direction respectively. From the results, the number of stories is still the most important factor and then follows the length and breadth. This result can be inferred in a similar manner as in case of the number of units prediction. But the importance of the factor number of stories is found to be less as compared to the number of units prediction as it is dependent mainly on the mass of the structure. The importance of length and breadth is found to be comparable to the number of units prediction as it has an influence on the mass of the building and the possible amount of spacing that can be provided between the damper units.

Figure 10.4 shows that the base shear is more or less only dependent on the effective stiffness of the base isolation system. All the other parameters are showing a negligible influence on the efficiency of prediction. The shear force at the base will primarily depend on the resistance offered by the building at the base. Hence by providing more effective stiffness, resistance offered by the building at the base is reduced. Thus, the machine can predict results by providing more importance to effective stiffness.

The feature importance for the time period shows that the output gives more or less equal importance to all the input parameters. The time period is a function of both the mass and stiffness of the building; hence mass is contributed by length, breadth and number of stories and the stiffness depends on the damper characteristics. Therefore, there is a need for considering more or less the same importance for all factors as shown in Figure 10.5.

The rank of the damper is predicted in such a way that the damper which can provide a maximum change in base shear is having a higher rank. Hence maximum shift of base shear can be achieved by providing the damper having optimum stiffness with respect to the building characteristics. Hence it is the damper properties is showing more importance in the prediction of output as shown in the Figure 10.6.

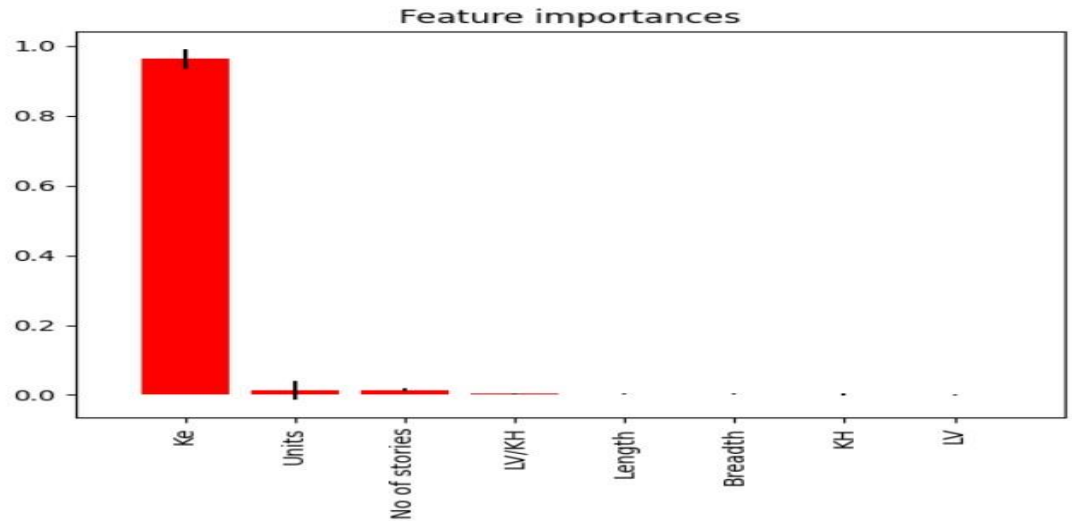

Figure 10.4 Feature importance for base shear

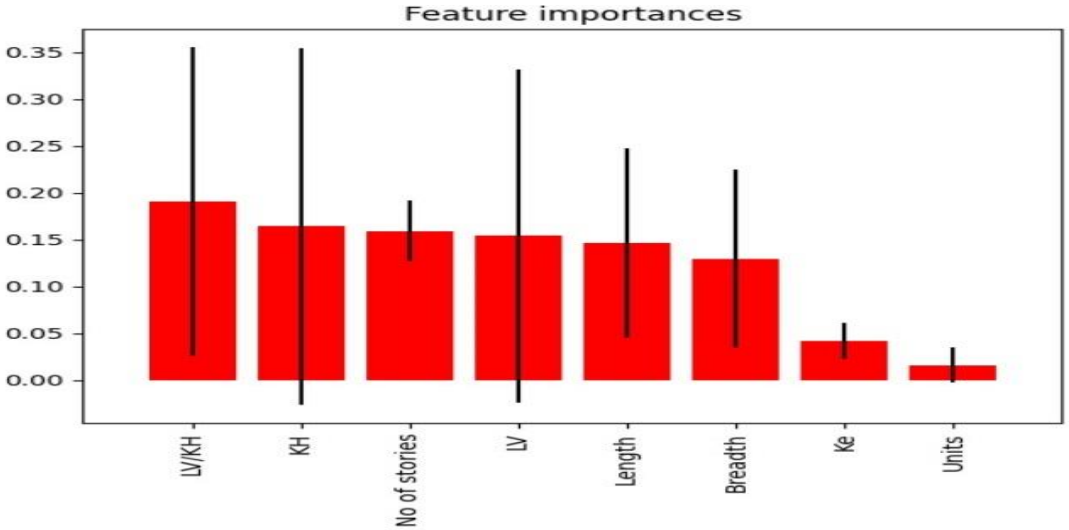

Figure 10.5 Feature importance for time period

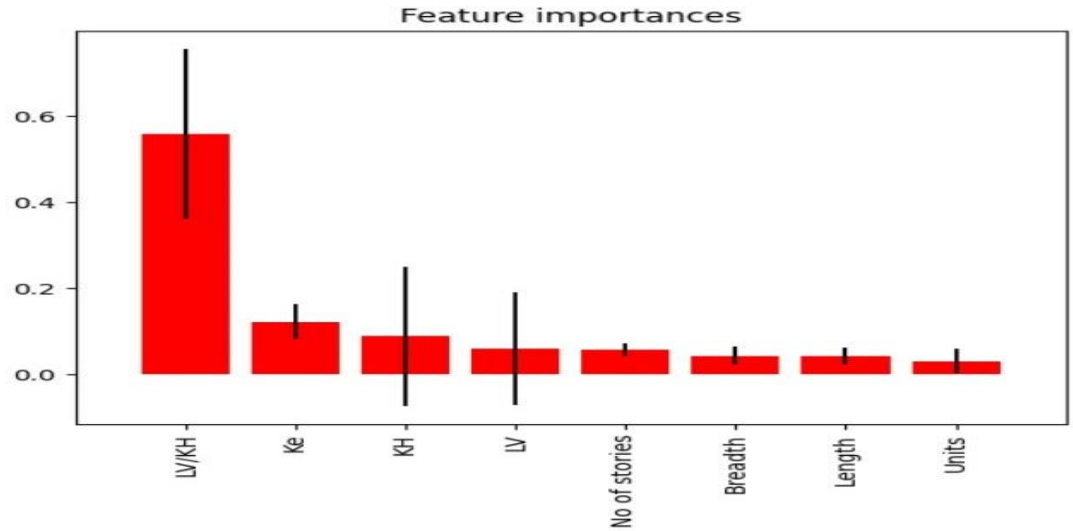

Figure 10.6 Feature importance for rank

Chapter 11

Performance Evaluation of ML Models

11.1. General

The performance evaluation is an important step in machine learning to analyse the quality of the prediction. It can be done by statistical evaluation metrics. Statistical analysis is a scientific instrument used in ML for capturing and analysing vast amounts of data in order to identify prominent trends and patterns and transform them into relevant information. It can thus be considered a technique that facilitates decision-making and enables us to anticipate the quality of predictions based on past trends. Hence in the present study performance of the proposed models is analysed in terms of statistical metrics and is explained in section 11.2 and the best model is suggested in terms of the evaluation scores.

11.2. Metrics Used for Valuation of ML Models

In the case of a Machine Learning model, it is very important to validate the performance of the models. The metrics continuously detect and it helps to quantify the quality of the results. As the present study deals with prediction, a regression model is used. The metrics used for the regression model include mean square error, coefficient of determination, root mean square, and mean absolute error. Hence these metrics are used to validate the results of the study.

Mean square error: It determines the squared average of the difference between the desired value and the value estimated by the regression model.

Root Mean Square Error: The Root Mean Square Error is the square root of the average squared difference between the desired value and the value estimated by the model.

R^2, Coefficient of determination: It is the degree of variability in the dependent output attribute that can be predicted from the independent input variables. Using the ratio of total deviation of results specified by the model, it is used to determine how well observed outcomes are reproduced by the model.

Mean Absolute Error: Mean Absolute Error is the mean difference between the actual and predicted values.

In the present study statistical evaluation of each parameter prediction is done in terms of MSE, RMSE, R^2, MAE.

11.3. Results and Discussion on Performance Evaluation

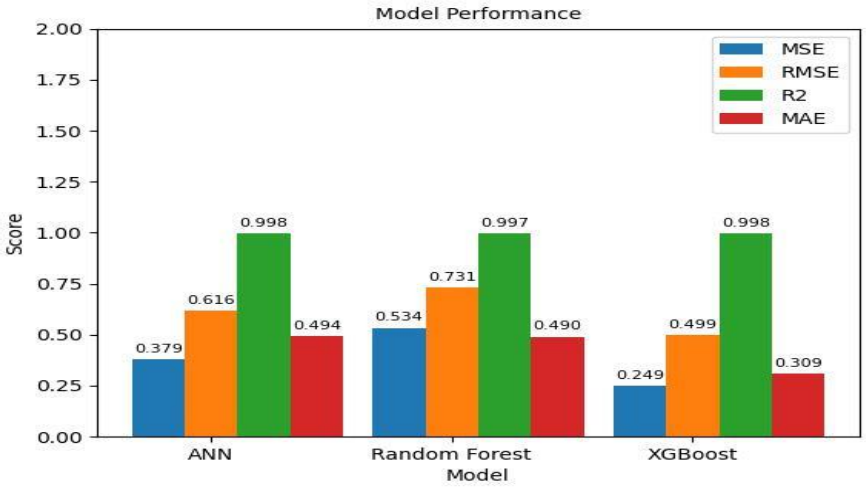

Figure 11.1 Model performance for the prediction of number of units

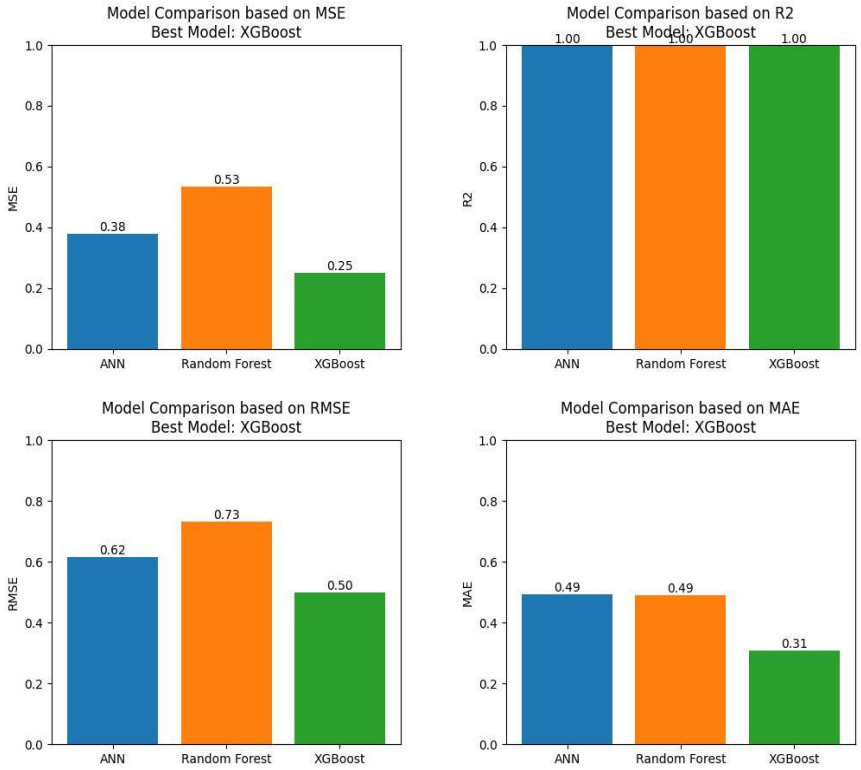

Figure 11.2 Statistical evaluation for the prediction of number of units

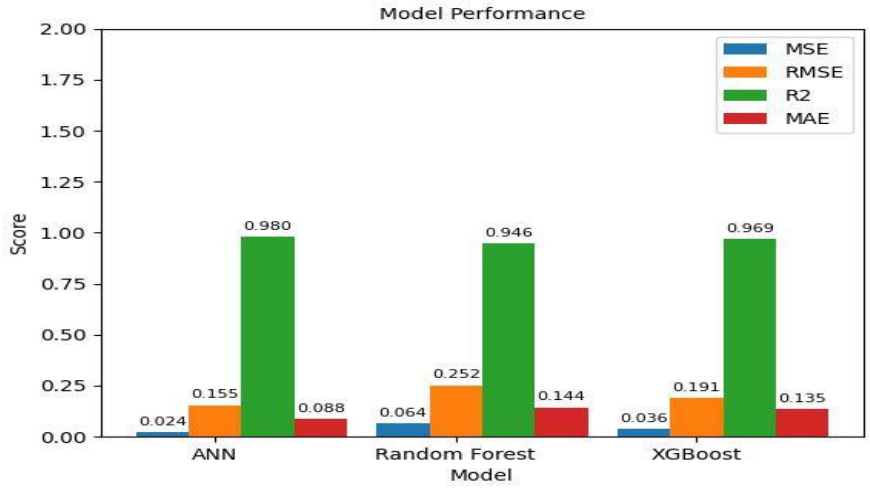

Figure 11.3 Model performance scores for spacing in x direction prediction

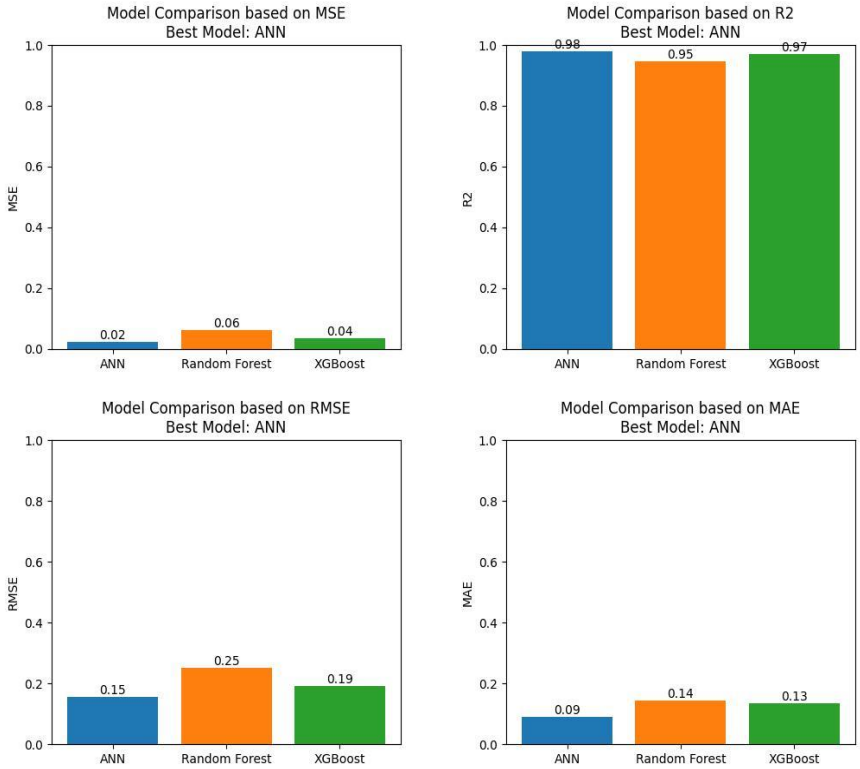

Figure 11.4 Statistical evaluation for the prediction of spacing in x direction

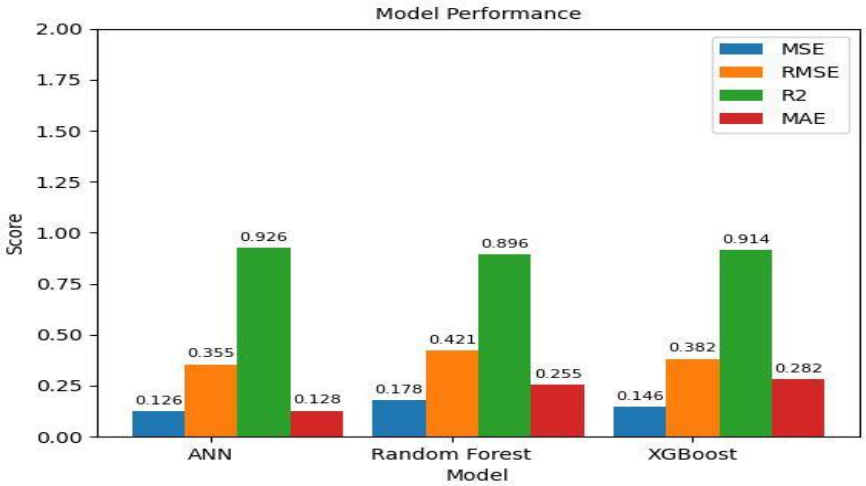

Figure 11.5 Model performance scores for spacing in y direction prediction

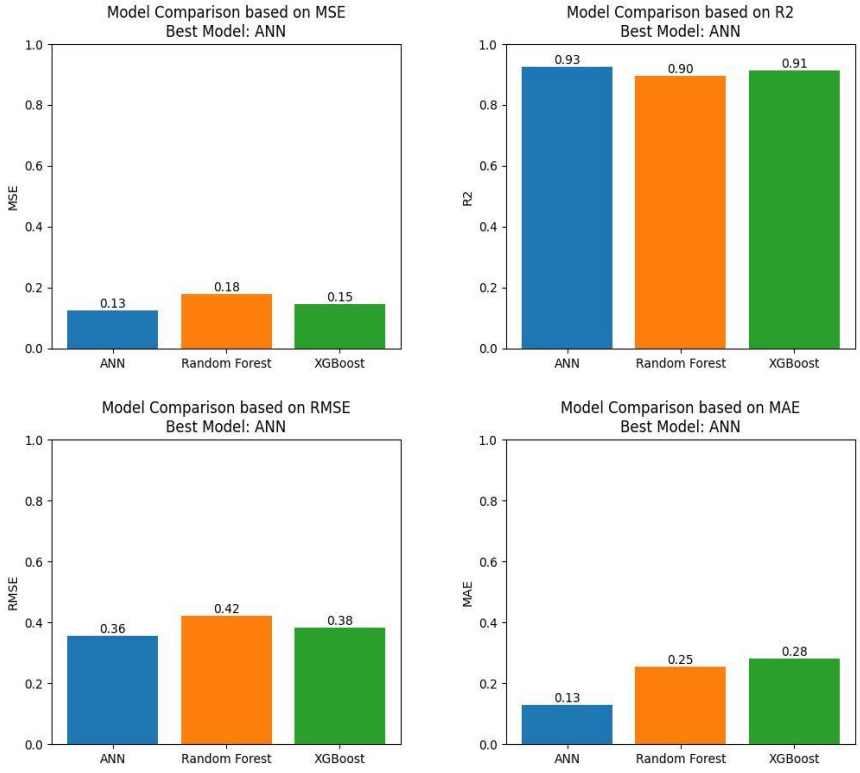

Figure 11.6 Statistical evaluation for the prediction of spacing in y direction

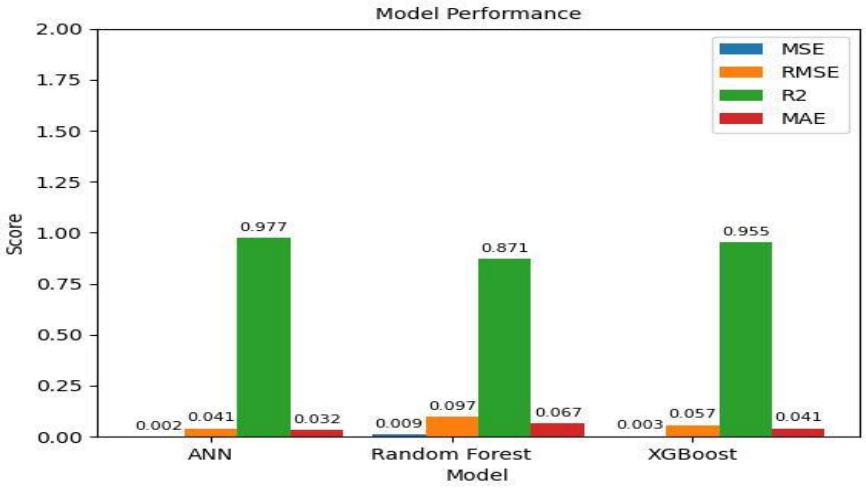

Figure 11.7 Model performance scores for time period prediction

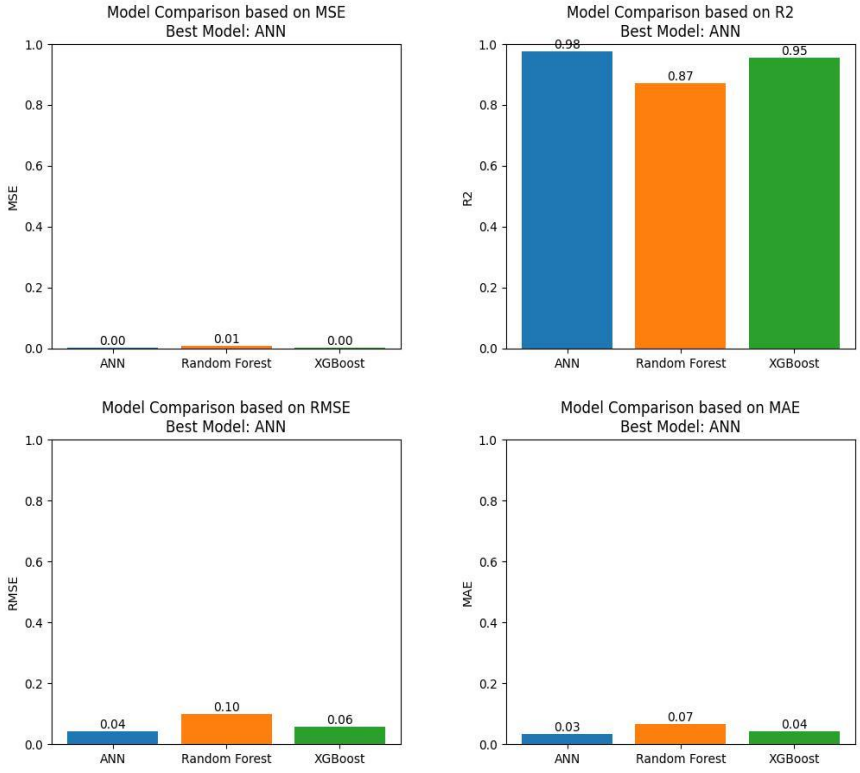

Figure 11.8 Statistical evaluation for the prediction of time period

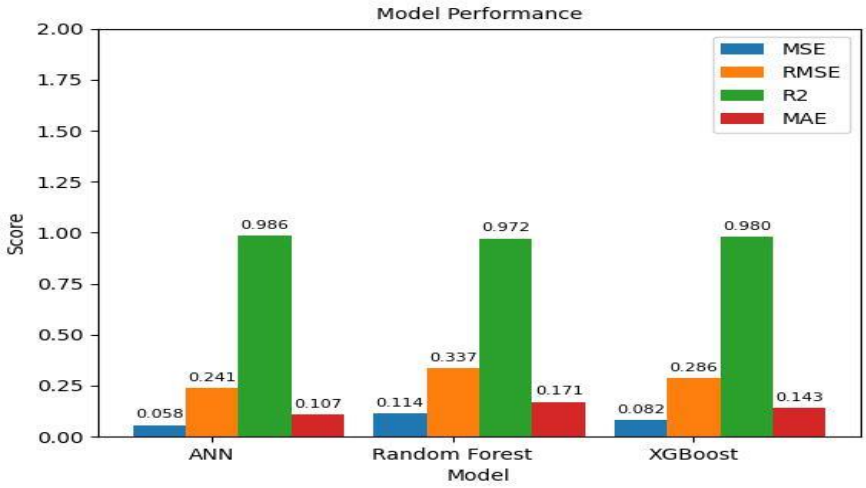

Figure 11.9 Model performance scores for base shear prediction

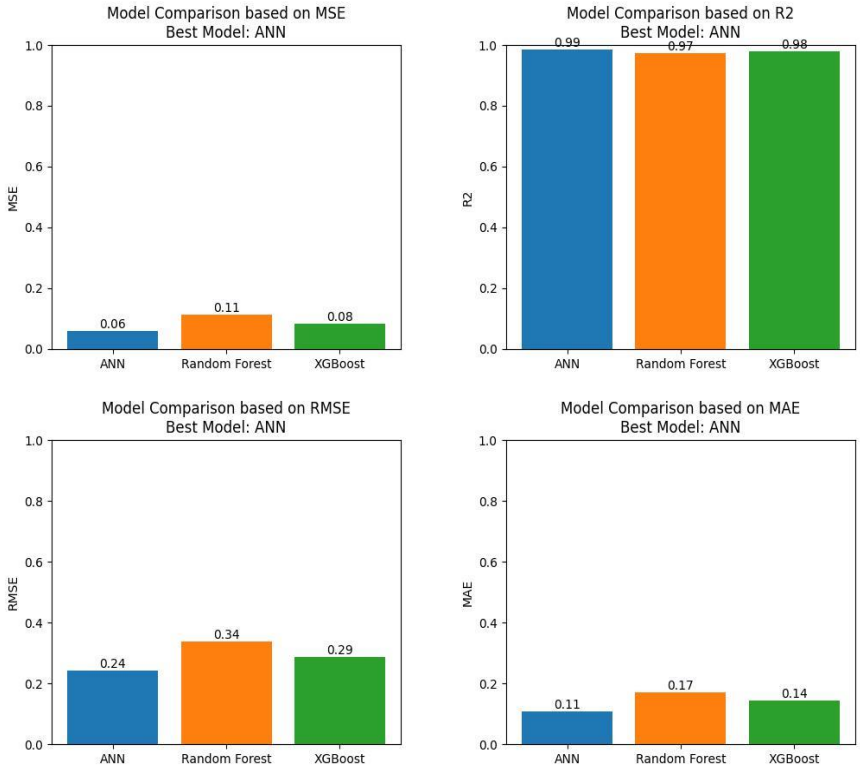

Figure 11.10 Statistical evaluation for the prediction of base shear

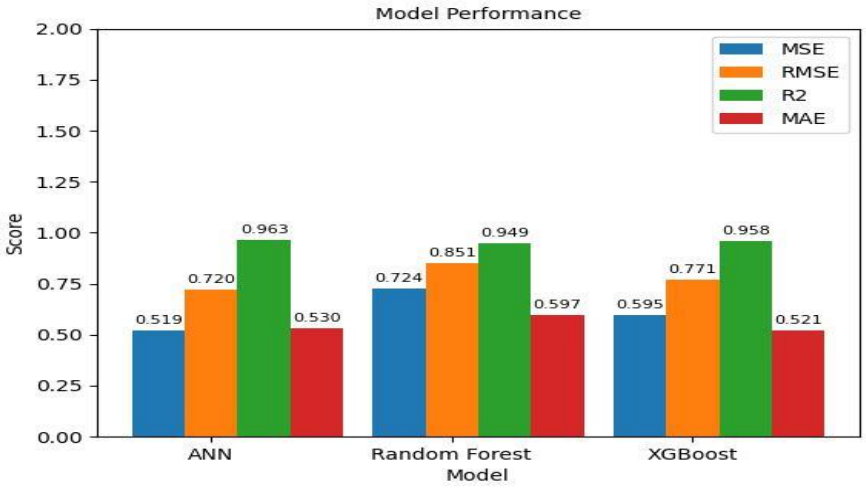

Figure 11.11 Model performance scores for rank prediction

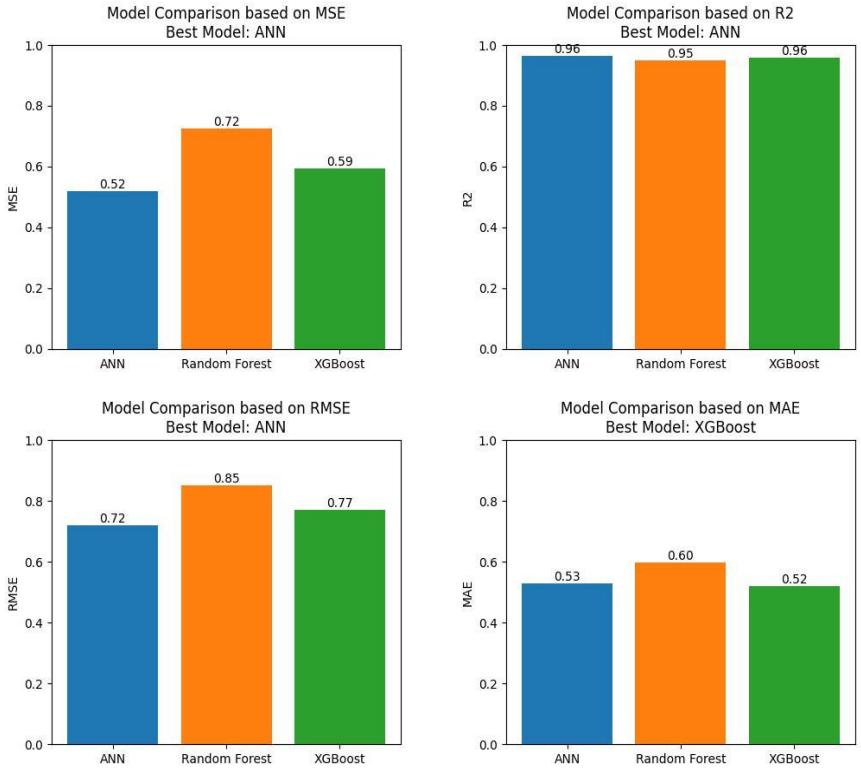

Figure 11.12 Statistical evaluation for the prediction of rank

The performance of the models is analysed as discussed in section 11.1 and using the metrics discussed in section 11.2. The prediction of the number of units is evaluated as shown in Figures 11.1 and 11.2. It implies that in the case of XG Boost model, the MSE value is 0.25 and the R^2 value yields similar results from all the models. As the RMSE value is found to be 0.5 and MAE value is 0.39 for the XG Boost model it seems to perform better than the other two models. Hence XG Boost can be considered as the best model in this case.

Figure 11.3 and 11.4 shows the value of the metrics for prediction of spacing in the x direction and Figure 11.5 and 11.6 shows the metric value for prediction of spacing in the y direction. The results show that all the models performed well in both cases. The three models had MSE, RMSE, and MAE values in the range of 0.25. The R^2 value of all the models in both cases also seems to be greater than 0.96 which is also appreciable. All three models performed exceptionally well in the case of time period prediction also as shown in Figures 11.7 and 11.8. The MSE, RMSE, and MAE values were found to be less than 0.1. But the performance of the Random Forest model in terms of coefficient of determination, R^2 seems to have a value less than 0.9 which is not good.

The MSE and MAE values for all the models in case of base shear prediction are found to be less than 0.11 which shows a very good performance. The R^2 value of all models seems to be greater than 0.98. When coming to the case of RMSE value the ANN is much better than other models as represented in Figures 11.9 and 11.10. Figure 11.11 and 11.12 shows the performance of the model in rank prediction. In this case, all the models have R^2 value in the range of 0.95, showing that the predicted values are in good fit with the trained value. The MSE score is better for ANN but the MAE is better in the case of XG Boost, by considering the scores of RMSE also ANN can be suggested as the best model for rank prediction.

By considering the overall performance the ANN can be considered as the best model. But the XG Boost performed better in the case of the number of units prediction more than ANN and seems to be the second best model from the study. The study shows that all the considered parameters can be effectively predicted by the three models out of which the prediction of the spacings, base shear and time period where more precise.

Chapter: 12

Conclusion

12.1. General

The study consists of the experimental analysis of the structural properties of the CSTP isolators along with the nonlinear time history analysis of unreinforced masonry structure with the CSTP isolator in ETABS software. From the experimental analysis, 12 set of dampers are proposed as explained in section 7.2. The shape factor of the specimen is varied by increasing the number of layers. The compression properties of the isolator are tested to study find the vertical stiffness of the CSTP specimen and its variation in vertical stiffness and compressive stress with change in shape factor is also investigated. To study the shear characteristic of the isolator under the seismic loading, the cyclic loading test is conducted. The influence of the shape factor on horizontal stiffness and damping ratio is studied. From the results obtained from the experimental analysis isolators are modelled in the ETABS software. Non-linear time history analysis is done with the El Centro earthquake as the input ground motion. By varying the number of stories and dimensions of the building, the performance of each of the 12 dampers where analysed as discussed in section 7.6. The ML models are then trained to predict the required number of damper units, its spacing, corresponding time period and base shear and the best damper combination in terms of rank as explained in chapter 11. The findings from the analysis can be summarized as follows

12.2. Compression Test

The load-deformation curve obtained from the compression testing of the CSTP specimens shows a load-deformation curve similar to the behaviour of a hardening spring. The experiment is conducted by increasing the number of layers, and it is found that the vertical stiffness is inversely proportional to the number of layers. After a certain loading, the stiffness of the isolator improves considerably in all cases under consideration. The tested CSTP specimens were observed to take considerable compressive stress, i.e., greater than 8 MPa, and were found to be in the range of 8–8.5 MPa. Hence, it is inferred that the variation of the shape factor doesn’t have a considerable effect on compressive strength.

12.3. Cyclic Load Test

The cyclic shear test is conducted to evaluate the lateral performance of the 12 sets of dampers. The lateral stiffness seems to increase with the increase in the shape factor, and the damping ratio is found to decrease with the increase in the shape factor. Hence, the lateral stiffness shall be reduced by decreasing the shape factor, but it may affect the stability of the isolator. The sliding between layers is observed in the case of a 10-layer 1 MPa sample. The dampers are found to be stiffer as the vertical pressure is increased. Hence, lateral stiffness is comparatively high for 3 MPa vertical pressure cases. From the experiment, it is also found that the damping ratio is inversely related to shape factor and vertical pressure. The experiment results show that the CSTPs can offer a damping factor in the range of 0.12 to 0.25, without any energy dissipation devices.

12.4. Numerical Analysis

Numerical analysis is performed in ETABS software by using EL Centro earthquake ground motion. A total of 324 models were analysed, including 288 models with base isolators and 36 plane frames. From the numerical results, it is observed that CSTPs can be effectively used as a base isolator. The performance of the base isolation system seems to be improved by providing the optimum number of damper units and spacings.

12.5. Feature Importance Study

The feature importance study is conducted to analyse the importance of each parameter that affects the desired output. The features that affect the number of units of dampers and spacing between the dampers are mainly the number of stories, length, and breadth of the building. The effective stiffness is found to be the feature that predominantly affects the base shear. The time period is found to be influenced to the same extent by all the input features, except the number of dampers. The feature that majorly affects rank prediction is found to be the vertical load-to-horizontal stiffness ratio.

12.6. Machine Learning Performance Evaluation

ML models can be effectively used to predict the parameters required for the CSTP base isolator design. The performance of models was found to be improved by tuning the hyperparameters of each model. The statistical evaluation of the models is done by using metrics like RMSE, R^2, MSE, and MAE, and their performance is compared. The ANN model exhibited the highest accuracy among the three developed ML models, and the XG Boost was found to be the second-best. In the prediction of the number of damper units,

XG Boost outperformed the ANN model. The performance of the models can be improved by increasing the amount of data in the dataset.

Chapter:13
Future Scope

- The study can be extended to unsymmetrical structures also.
- The ML models can be employed to predict the maximum displacement of the structure.
- The study can be done on reinforced cement concrete structures and steel structures.
- ML models could be used for the performance analysis of other isolators like lead rubber, friction pendulum etc.

References

1. Asim, K. M., et al. "Earthquake magnitude prediction in Hindukush region using machine learning techniques." *Natural Hazards* 85 (2017): Springer 471-486.
2. Basar, T., et al. "Seismic response control of low-rise unreinforced masonry building test model using low-cost and sustainable un-bonded scrap tyre isolator (U-STI)." *Soil Dynamics and Earthquake Engineering* 142 (2021), Elseveir: 106561
3. Calabrese, A., et al. "Recycled Rubber Fiber Reinforced Bearings (RR-FRBs) as base isolators for residential buildings in developing countries: The demonstration building of Pasir Badak, Indonesia." *Engineering Structures* 192 (2019) Elseveir: 126-144.
4. Dao, Nhan D., et al. "A new statistical equation for predicting nonlinear time history displacement of seismic isolation systems." *Structures*. Vol. 24. Elsevier, 2020.
5. Erduran, Emrah, Nhan D. Dao, and Keri L. Ryan. "Comparative response assessment of minimally compliant low-rise conventional and base-isolated steel frames." *Earthquake Engineering & Structural Dynamics* 40.10 (2011), Wiley online: 1123-1141.
6. Gavanski, Eri, Kurtis R. Gurley, and Gregory A. Kopp. "Uncertainties in the estimation of local peak pressures on low-rise buildings by using the Gumbel distribution fitting approach." *J. Struct. Eng* 142.11 (2016): 04016106.
7. Kelly, James M. "Seismic isolation systems for developing countries," *Earthquake Spectra 18*, no. 3,(2002).
8. Kiani, Jalal, Charles Camp, and Shahram Pezeshk. "On the application of machine learning techniques to derive seismic fragility curves." *Computers & Structures 218* (2019), Elseveir: 108-122.
9. Kitayama, Shoma, and Michael C. Constantinou. "Implications of strong earthquake ground motion duration on the response and testing of seismic isolation systems." *Earthquake Engineering & Structural Dynamics* 50.2 (2021), Wiley online: 290-308

10. Matsagar, Vasant A., and R. S. Jangid. "Base isolation for seismic retrofitting of structures." *Practice Periodical on Structural Design and Construction* 13.4 (2008): ASCE,175-185

11. Mishra, Huma Kanta, Akira Igarashi, and Hiroshi Matsushima. "Finite element analysis and experimental verification of the scrap tire rubber pad isolator." *Bulletin of Earthquake Engineering* 11.2 (2013), Springer: 687-707
12. Mousavi, S. Mostafa, and Gregory C. Beroza. "A machine-learning approach for earthquake magnitude estimation." *Geophysical Research Letters* 47.1 (2020): e2019GL085976.
13. Muñoz, André, Miguel A. Díaz, and Roy Reyna. "Applicability study of a low-cost seismic isolator prototype using recycled rubber." *Tecnia* 29.2 (2019): 65-73
14. Nguyen, Hoang D., Nhan D. Dao, and Myoungsu Shin. "Machine learning-based prediction for maximum displacement of seismic isolation systems." *Journal of Building Engineering* 51 (2022),Elseveir: 104251
15. Nguyen, Nam V., Hoang D. Nguyen, and Nhan D. Dao. "Machine learning models for predicting maximum displacement of triple pendulum isolation systems." *Engineering Structures* Vol. 36. Elsevier, 2022
16. Nguyen, Hoang D., et al. "Rapid seismic damage-state assessment of steel moment frames using machine learning." *Engineering Structures* 252 (2022): 113737
17. Nguyen, Hoang D., Nhan D. Dao, and Myoungsu Shin. "Prediction of seismic drift responses of planar steel moment frames using artificial neural network and extreme gradient boosting." *Engineering Structures* 242 (2021): 112518.
18. Ohsaki, Makoto, et al. "Finite-element analysis of laminated rubber bearing of building frame under seismic excitation." *Earthquake Engineering & Structural Dynamics* 44.11 (2015), Elseveir: 1881-1898
19. Pan P, Zamfi rescu D, Nakashima N, Nakayasu N and Kashiwa H. "Base-isolation design practice in Japan: introduction to the post-Kobe approach." Journal of Earthquake Engineering 9, no. 01,(2009)
20. Pauletta, Margherita, Andrea Cortesia, and Gaetano Russo. "Roll-out instability of small size fiber-reinforced elastomeric isolators in unbonded applications." *Engineering Structures* 102 (2015): 358-368

21. Raj, J. Cici Jennifer, and S. Suppiah. "Seismic isolation using scrap tire rubber pads." *Materials Today: Proceedings* 43 (2021) Elseveir: 1404-1407
22. Saedniya, Majid, and Sayed Behzad Talaeitaba. "Numerical modeling of elastomeric seismic isolators for determining force–displacement curve from cyclic loading." *International Journal of Advanced Structural Engineering* 11.3 (2019), Springer: 361-376
23. Shirai, Kazutaka, and Jihyun Park. "Use of scrap tire pads in vibration control system for seismic response reduction of buildings." *Bulletin of earthquake engineering* 18.5 (2020), Springer: 2497-2521
24. Sistla, Saiteja, and S. C. Mohan. "Parametric studies and application of fibre reinforced elastomeric isolators to low-rise buildings." *Structures*. Vol. 34. Elsevier, 2021
25. Tanwer,R ,Vya. “Comparative Study of Base Isolated Building with Fixed Base Building with Time History Analysis”.*International Journal for Research in Applied Science & Engineering Technology* (2019)
26. Tamim Tanwer, M., Tanveer Ahmed Kazi, and Mayank Desai. "A study on different types of base isolation system over fixed based." *Information and Communication Technology for Intelligent Systems*. Springer, Singapore, 2019. 725-734
27. S. K. Deb, A. Dutta, Thuyet and Van Ngo,. "Mitigation of seismic vulnerability of prototype low-rise masonry building using U-FREIs." *Journal of Performance of Constructed Facilities* 32.2 (2018), ASCE: 04017136
28. Turer, Ahmet, and Bayezid Özden. "Seismic base isolation using low-cost Scrap Tire Pads (STP)." *Materials and Structures* 41.5 (2008), Springer: 891-908
29. Zisan, M. B., and A. Igarashi. "Lateral load performance and seismic demand of unbonded scrap tire rubber pad base isolators." *Earthquake Engineering and Engineering Vibration* 20.3 (2021), Springer: 803-821.